

**ASSESSMENT OF HEAVY METAL CONCENTRATIONS AND  
RADIATION EXPOSURE DUE TO NATURALLY OCCURRING  
RADIOACTIVE MATERIALS IN THE LIMESTONE DEPOSITS OF KITUI  
SOUTH DISTRICT – KENYA.**

**By**

**Mulwa Bendibbie Munyao**

**A thesis submitted in the partial fulfilment of the requirement for the award  
of a Master of Science degree (MSc) in Physics, University of Nairobi**

University of NAIROBI Library



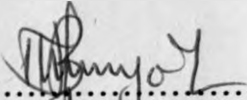
0378840 3

**2011**

## DECLARATION

This is my original work and has not been submitted for examination in any other university.

MULWA BENDIBBIE MUNYAO

Signature.....

Date.....20/07/2011.....

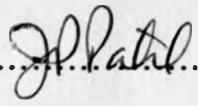
This thesis has been submitted for examination with the approval my supervisors:

1) Mr. D.M. Maina  
Institute of Nuclear Science and Technology  
University of Nairobi

Signature.....

Date.....19/7/11.....

2) Prof. J.P. Patel  
Department of Physics  
University of Nairobi

Signature.....

Date.....20.7.2011.....

# DEDICATION

To my mother, father, brothers, sisters, wife and friends.

ACKNOWLEDGMENTS

I wish to express my appreciation to the following for their assistance in the preparation of this manuscript: Dr. T. M. ... and Prof. ... The assistance of ... during the period of ...

1951

## **ACKNOWLEDGEMENTS**

I wish to express my sincere gratitude to my employer the Teachers Service Commission for granting me a study leave to pursue my studies. My supervisors Mr. D.M. Maina and Prof. J. P. Patel for their guidance throughout the research period. My thanks also go to Mr. Bartilol and Njogu both of The Institute of Nuclear Science and Technology for their assistance in practical work and to my wife Dorcus Mwende for her patience and encouragement during the period of my study.

## ABSTRACT

The heavy metals contents of Cu, Zn and Pb have been measured using Energy Dispersive X-Ray Fluorescence (EDXRF) and their pollution indexes calculated. The radiation background exposure at 1 m above the ground was measured using a survey meter and the annual effective doses and the absorbed dose rates calculated. The radioactivity levels of the limestone samples were also determined from the measurements done using a gamma ray spectrometry that consists of hyper pure germanium detector system. The results of measurements obtained indicated that heavy metal content in soils and limestone samples were generally below the soil metal limits given by U.S EPA with pollution indexes <1. The measured Annual effective dose rates averages of 0.768 mSv/yr, 0.907 mSv/yr and 0.743 mSv/yr, for Utekilawa- Kituvwi hills, Kamaluu-Mwanyani Hills and Ndulukuni Hills respectively which was below the recommended dose rate for the public (1mSv/yr) and the corresponding absorbed dose rates were 125.3 nGy/h, 147.82 nGy/h and 121.2 nGy/h which were about 2 times the average global absorbed dose rates. The area was therefore considered to be high background radiation area. The activity concentration measurements showed that  $^{238}\text{U}$  was the highest contributor to the background with a mean activity concentration of 28.34 Bq/Kg, 47.4 Bq/Kg and 32.24 Bq/Kg for Utekilawa- Kituvwi hills, Kamaluu-Mwanyani Hills and Ndulukuni Hills respectively while  $^{40}\text{K}$  had activity concentrations 95.58 Bq/Kg, 142.63 Bq/Kg and 87.35 Bq/Kg for samples from Utekilawa- Kituvwi hills, Kamaluu-Mwanyani Hills and Ndulukuni Hills respectively but  $^{232}\text{Th}$  was below detection limits for all the samples analysed. The contribution for the effective doses as a result of radionuclides in limestone were 0.047 mSv/yr (6%), 0.088 mSv/yr (10%) and 0.064 mSv/yr (9%) Utekilawa- Kituvwi hills, Kamaluu-Mwanyani Hills and Ndulukuni Hills respectively which was considered insignificant in the use of building materials made from the limestone.

## **TABLE OF CONTENTS**

**Page**

DECLARATION.....	ii
DEDICATION.....	iii
ACKNOWLEDGEMENTS.....	iv
ABSTRACT.....	v
TABLE OF CONTENTS.....	vi
LIST OF FIGURES.....	ix
LIST OF TABLES.....	x
LIST OF ABBREVIATIONS AND ACCRONYMS.....	xi

### **CHAPTER ONE: INTRODUCTION Pages 1-8**

1.0 Introduction.....	1
1.1 Sources of Ionizing Radiation in the Environment.....	1
1.2 Mining and Heavy Metals.....	4
1.3 Geology of Kitui South .....	5
1.4 Statement of the Problem.....	7
1.5 Objectives.....	7
1.6 Justification and Significance of the Research.....	8

### **CHAPTER TWO: LITERATURE REVIEW Pages 9-15**

2.1 Mining and Exposure to Ionizing Radiations.....	9
2.2 Limestone Mining and Radiation Exposure.....	12
2.3 Mineral Mining and Heavy Metals.....	14

## **CHAPTER THREE: THEORETICAL BACKGROUND Pages 16-26**

3.0 Introduction.....	16
3.1 Energy Dispersive X-Ray Fluorescence (EDXRF) Analysis.....	16
3.1.1 Matrix Effects.....	19
3.1.2 Matrix Correction Method for Transparent Sample Analysis.....	20
3.2 Interaction of Gamma Rays with Matter.....	23
3.2.1 Mechanisms of Interaction.....	23
3.3 Absorbed Gamma Dose Rates, Activity Concentrations AEDs.....	25

## **CHAPTER FOUR: MATERIALS AND METHODS Pages 27-32**

4.0 Introduction.....	27
4.1 Study Area.....	27
4.2 Sampling.....	27
4.3 Energy Dispersive X-Ray Fluorescence Spectrometric Analysis.....	28
4.4 EDXRF Procedures.....	28
4.5 Measurement of External Gamma Doses and External Effective Doses in Air.....	29
4.6 Measurements of Activity Concentrations .....	30
4.7 Gamma Ray Spectrometry.....	31

## **CHAPTER FIVE: RESULTS AND DISCUSSION Pages 33-61**

5.0 Introduction.....	33
5.1 Elemental Analysis.....	33
5.1.1 Region 1(Utekilawa-Kituvwi Hills).....	33
5.1.2 Region 2 (Kamaluu- Mwanyani Hills).....	39
5.1.3 Region 3 (Ndulukuni Hills).....	45
5.2 Absorbed Dose Rates and Annual Effective Dose Rates.....	51
5.2.1 Region 1(Kituvwi-Utekilawa Hills).....	52
5.2.2 Region 2 (Kamaluu-Mwanyani Hills).....	55
5.2.3 Region 3 (Ndulukuni Hills).....	58

**CHAPTER SIX: CONCLUSIONS AND RECOMMENDATIONS Pages 62-63**

REFERENCES.....	64
APPENDICES.....	70
Appendix 1: Absorbed Dose and AEDs for Samples from Utekilawa-Kituvwi Hills	70
Appendix 2: Absorbed Dose and AEDs for Limestone from Kamaluu-Mwanyani Hills	71
Appendix 3: Absorbed Dose and AEDs for Limestone Samples from Ndulukuni Hills	72



<b>LIST OF FIGURES</b>		<b>Page</b>
Figure 2.1	Geological map of Kitui South	6
Figure 3.1	Experimental procedure for matrix absorption correction	21
Figure 4.1	Block diagram of EDXRF spectrometry	28
Figure 4.2	Block diagram of HPGe spectrometry	32
Figure 5.1:	Annual Effective Dose rates for Utekilawa-Kituvwi	54
Figure 5.2:	Absorbed dose rates for Utekilawa-Kituvwi	54
Figure 5.3:	Absorbed dose rates for Kamaluu-Mwanyani Hills	57
Figure 5.4:	Annual Effective Dose rates for Kamaluu-Mwanyani	57
Figure 5.5:	Annual Effective dose rates for Ndulukuni Hills	60
Figure 5.6:	Absorbed dose rates for Ndulukuni Hills	60

<b>LIST OF TABLES</b>	<b>Pages</b>
Table 5.1: Metal concentration for soil samples from Utekilwa-Kituvwi Hills	34
Table 5.2: Heavy Metal Pollution Indexes for Soils from Utekilawa-Kituvwi Hills	35
Table 5.3: Metal Concentration for Limestone Samples from Utekilwa-Kituvwi Hills	37
Table 5.4 Limestone Pollution Indexes for Soils from Utekilawa-Kituvwi Hills	38
Table 5.5 Metal Concentration for Soil Samples from Kamaluu-Mwanyani Hills	40
Table 5.6: Soil Pollution Indexes for Soils from Kamaluu-Mwanyani Hills	41
Table 5.7: Metal Concentration for Limestone in Kamaluu-Mwanyani Hills	43
Table 5.8: Metal pollution indexes for limestone from Kamaluu-Mwanyani Hills	44
Table 5.9: Metal concentration for Soil samples in Ndulukuni Hills	46
Table 5.10: Metal pollution indexes for soil samples in Ndulukuni Hills	47
Table 5.11: Average metal concentration for limestone samples from Ndulukuni Hills	49
Table 5.12: Metal pollution indexes for limestone samples in Ndulukuni Hills	50
Table 5.13: Activity concentrations for Limestone from Kamaluu-Mwanyani Hills	53
Table 5.14 Activity Concentrations of Limestone from Kamaluu-Mwanyani Hills	56
Table 5.15: Activity Concentrations of Limestone Samples from Ndulukuni Hills	59

## **LIST OF ABBREVIATIONS AND ACCRONYMS**

<b>AED:</b>	<b>Annual Effective Dose rates</b>
<b>AXIL:</b>	<b>Analysis of X-ray Spectra by Iterative Least Squares fitting</b>
<b>EC:</b>	<b>European Commission</b>
<b>EDXRF:</b>	<b>Energy Dispersive X-ray Fluorescence</b>
<b>EURATOM:</b>	<b>European Atomic Energy Community</b>
<b>FWHM:</b>	<b>Full Width at Half Maximum</b>
<b>HBRA:</b>	<b>High Background Radiation Area</b>
<b>HLNRA:</b>	<b>High Level Natural Radiation Area</b>
<b>IAEA:</b>	<b>International Atomic Energy Agency</b>
<b>ICRP:</b>	<b>International Commission on Radiation Protection</b>
<b>MAD:</b>	<b>Maximum Annual Effective Dose</b>
<b>MCA:</b>	<b>Multichannel Analyzer</b>
<b>NCRP:</b>	<b>National Council on Radiation Protection</b>
<b>NORM:</b>	<b>Naturally Occurring Radioactive Materials</b>
<b>TENORM:</b>	<b>Technologically Enhanced Naturally Occurring Radioactive Materials</b>

# CHAPTER ONE

## INTRODUCTION

### 1.0 Introduction

This chapter discusses the background information of the present study; the sources of radionuclides, the effects of ionizing radiations from the primordial radionuclides, cosmic radiations as well as how the human activities affect the concentrations of these radionuclides. The different types of Naturally Occuring Radioactive Materials (NORM) and Technologically Enhanced Naturally Occuring Radioactive Materials (TENORM) together with their sources and the effects of mining on the enhancement and distribution of heavy metals.

### 1.1 Sources of Ionizing Radiation in the Environment

There are two main sources of background radiations in the atmosphere; naturally occurring radioactive materials (NORM) and cosmic radiations entering the atmosphere from the upper atmosphere originating from the sun. The NORM exists in soils and rocks. Traces of natural radionuclides  $^{238}\text{U}$ ,  $^{232}\text{Th}$  and  $^{40}\text{K}$  are present in water, soil, air, plants and animals' tissues and form the background radiation sources in the environment.

Over long periods several natural processes such as weathering, faulting, folding etc makes these NORM to exist in various geological formations in soils and rocks. Human beings are therefore always subjected to the risk of internal exposure to these ionizing radiations through ingestion of food, water and air as well as cosmic rays from the sun. These radionuclides can enter the food chain due to the solubility of their oxides thus being available in water, plants and animals (Malance *et al*, 1996; Aly- Abdo *et al*, Ibraheim *et al*, 1993).

Human activities such as mining, medical diagnostic and therapeutic procedures, mineral processing, nuclear power generating etc, may lead to increased exposure to naturally occurring radioactive materials called Technologically Enhanced Naturally Occuring Radioactive Materials (TENORM) (Juhašz *et al*, 2005). This has lead to a large number of workers being exposed to ionizing radiations. According to a report (UNSCEAR, 2008), about 22.8 million

workers are exposed to ionizing radiation with about 13 million being exposed to natural sources and about 9.8 million to artificial sources. However due to the rapid increase in human activities this number is expected to increase tremendously.

International guidelines and directives for dealing with exposure due to (NORM) exist, though only a few countries have adopted them and made regulations for their recommended limits of exposure for workers and the general public (ICRP, 2000; NCRP, 1993). The European Atomic Energy Community (EURATOM) (EC, 2002) and International Atomic Energy Agency (IAEA, 2004) also recommended exemption levels in activity concentrations for substances containing the NORM.

Based on the risk factors, the International Commission on Radiation Protection (ICRP) has published recommendations for dose limits for occupational exposure (workers) and the general public. The recommended effective dose limit is 20mSv per year averaged over five years (100mSv cumulative dose) and not to exceed 50mSv in a given year for radiation workers. For the general public, the recommended annual effective dose limit is 1mSv per year (ICRP, 1991).

Terrestrial natural sources of radiations vary greatly from place to place. Different studies have shown high levels of natural background radiation in many areas of the world; In Guangdong province China (Wei *et al*, 1993), South west coast of India (Sunta, 1990), Ramsar area in the Republic of Iran (Sohrabi, 1990), and Mrima hills of South coast Kenya (Patel, 1991). These high levels of background radiation are due to the occurrence of anomalous concentrations of the naturally occurring radionuclides in the environment, i.e. rock, soil, water etc.

The other natural components of background radiation include cosmic rays and radiation from cosmogenic radionuclides. Cosmic radiation refers to both the primary energetic radiation from solar and galactic events. When the primary radiation showers the earth's atmosphere, they undergo reactions and transform to secondary radiation.

Annual external dose rates from cosmic rays depend partly on latitude and altitude. The latitude effect is due to the charged particle nature of the primary cosmic rays. When they come near the earth, its magnetic field tends to deflect the rays away from the equator and lower latitudes, and the deflection reduces toward the poles (UNSCEAR, 2000; Rasolonjatovo *et al*, 2002). For example, at latitudes lower than  $30^{\circ}$ , the average external dose from cosmic radiation is

$305\mu\text{Svyr}^{-1}$  and approximately greater than  $350\mu\text{Svyr}^{-1}$  at latitudes higher than  $50^{\circ}$  north and south of the equator. The average values also increase from  $340\mu\text{Svyr}^{-1}$  at sea levels to  $460\mu\text{Svyr}^{-1}$  at 1000m above sea level (UNSCEAR, 2000; Rasolonjatovo *et al*, 2002).

The terrestrial component of the natural background radiation is dependent on the composition of soils and rock which typically contain natural radionuclides. Determination of soil radioactivity is essential for understanding changes in the natural radiation background (Tzortzis *et al*, 2004). Soil generally contains small quantities of the radioactive elements, uranium and thorium along with their progeny. Primordial radionuclides that are a source of external radiation are  $^{238}\text{U}$  and  $^{232}\text{Th}$  series  $^{40}\text{K}$ . Although  $^{235}\text{U}$  exists in soils, it accounts for very small quantities in the human body. Variation of natural radioactivity of soil depends on type, moisture content, and in homogeneity of its permeability (Varley and Flowers, 1998), formation, transports processes and geomorphology (El-Arabi, 2005) associated with meteorological conditions. Soil formation and chemical and biochemical interactions also influence the distribution patterns of uranium, thorium and their decay products (Karakelle *et al*, 2002).

Environmental radiation monitoring of soil samples is crucial to determine the radioactivity levels and evaluate the doses at sites around a mining /extraction or mineral processing plant before and after the plant construction. Such monitoring is useful for evaluating possible impacts to public health and the natural environment before plant construction and ensuring normality during its commercial operations (Tsai, *et al* 2008)

Mining activities can cause deleterious effects on the environment due to deposition of large amounts of waste on the soil. These negative effects on the environment caused by mining activities are mainly due to presence of high volumes of tailings (Dudka and Adriano, 1997). These tailings usually have unfavorable conditions to natural vegetation growth such as acidity (Wong, 1998), high concentrations of heavy metals (Norland and Veith, 1995), low water retention capacity (Henriques and Fernandes, 1991) and low levels of plant nutrients (Wong, 2003). All these factors make mine tailings, sources of pollution to ground and surface waters and soils (Conesa *et al*, 2006).

## 1.2 Mining and Heavy Metals

Limestone is a mineral that is mined and processed in Kenya and used for making cement and other building materials. Discovery of large deposits of limestone in Kitale South district of Kenya has attracted many companies interested in limestone mining and processing. No studies have been carried out on the potential risks of the extraction and processing of this limestone.

The environmental effects due to mining activities have been studied worldwide. A study of heavy metal concentration in growth bands of corals showed higher levels of Cu, Zn, Mn and Fe derived from mine tailings in Merinduque Island-Philippines (David, 2003). Heavy metal toxicity assessment using biotest in South Morocco showed very high heavy metal concentration with Zn concentration (38000-10800 mg/Kg), Pb (20412- 30000 mg/Kg), Cu (2019-8635 mg/Kg) and Cd (148 -228 mg/Kg). The soil pH values in the same region also had wide variations ( 2.6-8.8), (Boularbah, 2006). In Spain, a study on distribution of Heavy metals from mine wastes from an old Pb-Zn mine showed very high concentrations of metal ions i.e. 28453.50 mg/Kg for  $Pb^{2+}$ , 7000.44 mg/Kg for  $Zn^{2+}$ , 20.87 mg/Kg for  $Cd^{2+}$  and 308.48 mg/Kg for  $Cu^{2+}$ . High concentrations of Pb, Zn and Cd were also found in many of the samples taken from the arable and pasture land surrounding the mine indicating a certain extent of spreading of heavy metal pollution (Rodriquez *et al*, 2009).

Exposure to radiation of the public near the site may arise from radionuclides which may be directly ingested through food chain or from the re-use of mine wastes. This research is aimed at providing information on possible radiological exposure risks as well as pollution effects which will result from limestone mining when the commercial extraction begins.

### 1.3 Geology of Kitui South

The rocks of Kitui South fall into three main groups: Proterozoic age rocks of basement system, the tertiary Yatta plateau phonolite and superficial deposits of Pleistocene to the recent years. The basement rocks are mainly metamorphosed sediments now altered to marbles, gneisses and granulites (Saggerson, 1957). Tertiary phonolite forms patches that outcrop in the southwest corner of the area and represent small tongues of the main Yatta plateau lava which poured out in the area to west along fissures aligned North-West to South- East as shown in figure 1 (Dodson, 1953). Superficial sands, gravels and soils are extensive over the whole area and almost conceal the underlying rocks on the end of the tertiary peneplane. Black cotton soil is present west of the main North-South road, whilst superficial Kunkar limestone deposits are scattered and rare.

The crystalline limestone outcrops in the area and the major bands are continuous over considerable distances. The major bands are found in the Kitui- Kanziku hills and have probably been repeated by folding and faulting although there is undoubtedly more than one horizon present. One horizon in the area six miles west of Kanziku is probably continuous as far north as Musa near Ikanga. In Kanziku graphite bands are formed near the base of the marble, many bands occur within and throughout the marble horizon. The marbles, where seen in outcrops consist principally of calcite and recrystallization of limestone is evident where extremely coarse calcite crystals occur, as at Ndulukuni, see in figure 1 (Saggerson, 1957). The area has three main limestone deposits: Kituvwi-Utekilawa hills, Kamaluu-Mwanyani hills and Ndulukuni as indicated in Figure 1.1 (Saggerson E.P, 1952).



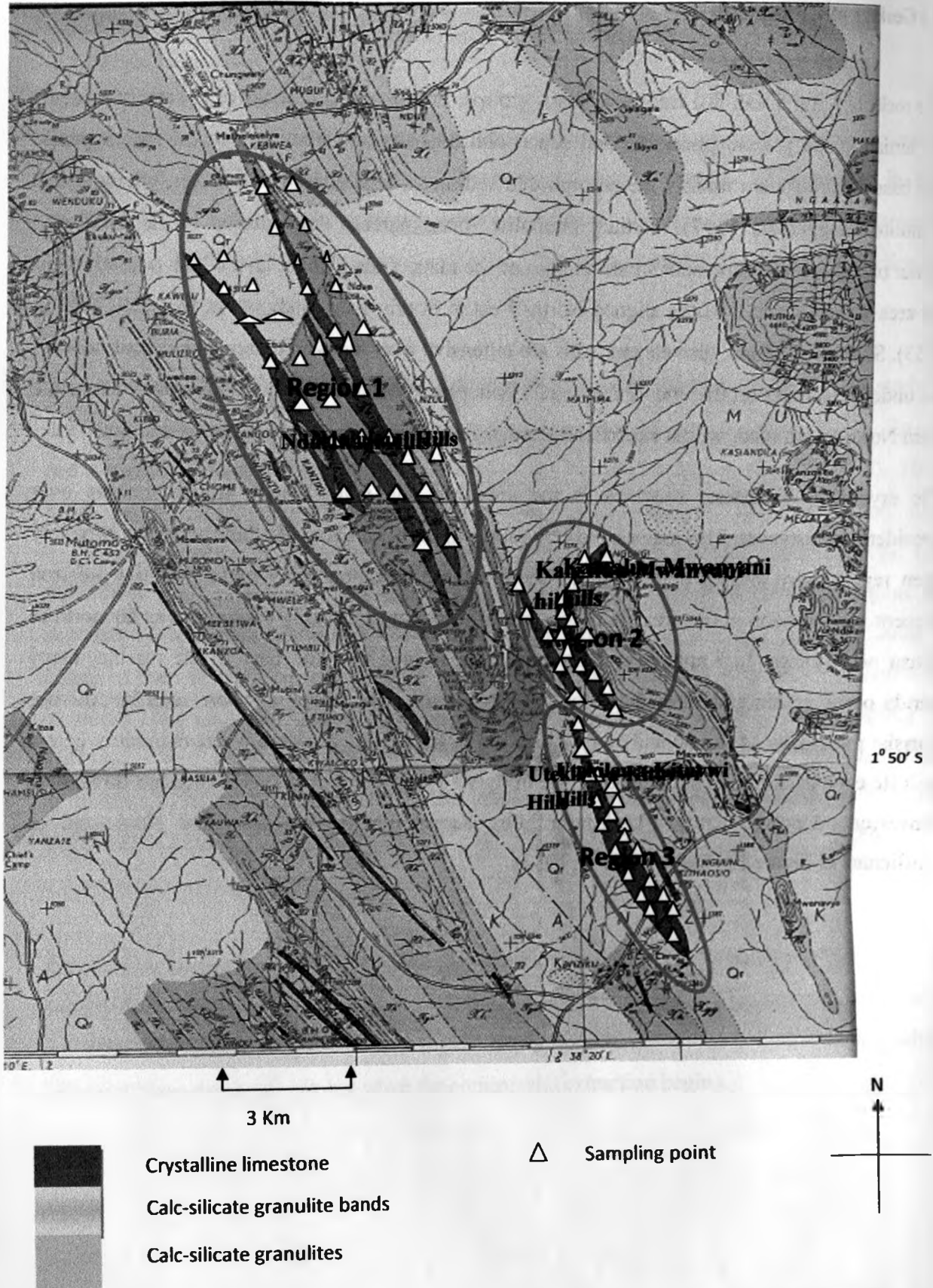


**Figure 1.1: Simplified Geological map and sampling sites of Kitui South (Saggerson, E.P 1952)**

#### **1.4 Statement of the Problem**

No research has been carried out concerning naturally occurring radioactive materials (NORM) as well as concentration and distribution of heavy metals in the local environment in Kitui south district of Kenya. However, building materials such as bricks are made from these soils. The discovery of huge limestone deposits in this region has attracted limestone mining /extraction and cement manufacturing companies which are currently in the process of setting up plants in the region. This is a likely source of uncontrolled exposure to ionizing radiation and heavy metals contamination associated with limestone ore when commercial extraction and processing of the limestone operations start.

#### **1.5 Objectives**

The main purpose is to provide relevant data on the presence and quantities of radioactive elements, exposure levels to ionizing radiation and heavy metals associated with the limestone deposits of Kitui South district of Kenya.

##### **1.5.1 Specific Objectives**

1. To determine the radioactivity levels of naturally occurring radio-nuclides i.e  $^{40}\text{K}$ ,  $^{238}\text{U}$  and  $^{232}\text{Th}$  in limestone ore in Kitui South.
2. To determine the concentration levels of heavy toxic elements such as Zn, Pb, Cu etc in limestone and soil samples in Kitui South.
3. To determine the effective dose rates and absorbed dose rates in the ambient atmosphere.
4. To determine the effective doses and absorbed dose rates from the measurements of activity concentrations of radionuclides in limestone samples of Kitui South.

## **1.6 Justification and Significance of the Research**

Mining activities have been associated with the exposure to radionuclides and heavy elements in the mineral ores due to disposal of large amount of tailings (Dudka and Adriano, 1997). The results of this research are expected to form a data for exposure levels.

The data base will serve to create awareness to general public, legislators, regulators and the general public about the radiological exposures due to NORM in the region and of heavy metals contamination and distribution in the soils. The information obtained will form an important reference for monitoring the effect of limestone mining activities to the environment, hence, provide basis for controlled exposure as well as disposal of the industrial wastes and mine tailings. No research as to the presence and distribution of both radio-nuclides and heavy toxic elements in Kitui South has been done.

## CHAPTER TWO

### LITERATURE REVIEW

#### 2.1 Mining and Exposure to Ionizing Radiations

The existence of High-Level Natural Radiation Areas (HLNRAs) is attributed to the availability of certain radioactive minerals or elements embedded in the continental rock system of these. Some mineral ores contain radionuclides of natural terrestrial origin commonly referred to as primordial radionuclides. These are mainly  $^{238}\text{U}$  and  $^{232}\text{Th}$  and their decay products and  $^{40}\text{K}$ . The activity concentrations of radionuclides in normal rocks and soils are variable but generally low. However, some commercially exploited minerals contain high levels of radionuclides (Odumo, 2009).

Activities associated with extraction, processing and use of minerals have the potential to cause exposures to ionizing radiation to the members of the general public and workers. This is due to the enhanced levels of the natural radionuclides in the processed ore, depending on the type of the industrial process used in the milling of the main ore and the presence of some radionuclides associated to the main ore. This is the so called Technologically Enhanced Naturally Occurring Radioactive Materials (TENORM).

Zircon is a mineral that is widely used in the ceramic industry. A radiological study on a Zircon milling plant showed total effective dose rates that were nearly the maximum recommended of  $1\text{mSv/yr}$  for the members of public. Due to this the authors recommended careful monitoring and control of the industry (Ballesteros *et al*, 2008).

Ilmenite and Amang have also been assessed for their radioactive materials content. A radiological impact assessment on effect on the environment in an Amang processing plant at Dengkil, Selengor, Malaysia on doses received by the public as well as occupational doses was done with the assumption that the area will be converted to a residential or industrial region once the plant is closed (Azlina *et al*, 2003). The predicted maximum annual effective dose rates for residents and industrial workers were  $1.94\text{mSvyr}^{-1}$  to  $10.41\text{mSvyr}^{-1}$  and  $35.03\text{mSvyr}^{-1}$  to  $35.0\text{mSvyr}^{-1}$  respectively each exceeding the maximum recommended values.

The activity concentration of  $^{238}\text{U}$  and  $^{232}\text{Th}$  in soils and mineral sands from the Nigerian tin mine of Bisichi area located in Jos plateau were done using HPGe detector. The activity concentrations in Bisichi ranged from  $8.7\text{kBq Kg}^{-1}$  to  $51\text{kBq Kg}^{-1}$  and  $16.8\text{kBq Kg}^{-1}$  to  $98\text{kBq Kg}^{-1}$  from  $^{238}\text{U}$  and  $^{232}\text{Th}$  respectively. These values were significantly high for areas of high natural radioactive background. The study also showed radionuclide concentrations in foodstuffs and water in samples to exceed the UNSCEAR reference values (Arogunjo *et al.*, 2008).

Funtua and Elegba (2005) estimated the radiological impact of the processing of cassiterite and Columbite from different mills of Jos Plateau (central Nigeria). (Funtua and Elegba, 2005). The results indicated that the average dose rate at different processing points and locations at the mills had values ranging from  $5\ \mu\text{Sv h}^{-1}$  for the background in the premises to  $80\ \mu\text{Sv h}^{-1}$  for that of processed zircon. Assuming a 2000-h working year, workers in the processing mills were exposed to an annual dose of about  $10\text{mSv}$  for the background and an average of  $160\text{mSv}$  for processed zircon, far above the  $20\text{mSv}$  annual dose limit. The dose rates of about  $25\ \mu\text{Sv h}^{-1}$  measured for the tailings gave an annual dose of about  $50\text{mSv}$  for a non radiation worker in the vicinity of the milling plant, exceeding the  $1\text{mSv year}^{-1}$  dose limit for the members of the public.

In Egyptian pyramids and tombs in the Saggara area, measurements of radon ( $^{222}\text{Rn}$ ) and its progeny, as well as thorium ( $^{232}\text{Th}$ ) progeny were made and the results used in calculation of the maximum annual effective dose (MAD) and other important occupational radiation exposure variables. It was found that for the limited time to which occupational workers and visitors were exposed, their respective MAD values were lower than those recommended by ICRP (i.e.,  $20\text{mSv}$  per year for occupational workers and  $1\text{mSv}$  in a year for the public). However, it was shown that if the exposure times for occupational workers at three archaeological sites were to increase to normal working schedules their MAD would be exceeded. Implementation of improved ventilation practices was recommended in those sites to reduce the exposure to occupational workers (Bigu *et al.*, 2000).

Mbuzukongira, (2006) analyzed coltan samples from Congo using Gamma-ray spectrometry for activity concentration of  $^{226}\text{Ra}$  and  $^{232}\text{Th}$ . In most of the samples analysed,  $^{40}\text{K}$  was below

detection limit which was calculated to be 0.141Bq/g considering a counting time of 20 hours (72000 seconds). All the Coltan samples contained activity concentrations of  $^{226}\text{Ra}$  and  $^{232}\text{Th}$  (i.e average activity concentration ranging from 0.32 to 1.56 Bqg<sup>-1</sup> for  $^{232}\text{Th}$  and 3.87 to 13.45 Bqg<sup>-1</sup> for  $^{226}\text{Ra}$ ) that were much higher than the normal concentrations found in typical soil and rock samples (0.01 to 0.05 Bqg<sup>-1</sup> for  $^{226}\text{Ra}$  and 0.007 to 0.05 Bqg<sup>-1</sup> for  $^{232}\text{Th}$ ). Effective dose from digging and the total dose to miners who dig Coltan were calculated (Mbuzukongira, 2006). The calculated values varied widely (from 0.007 to 18.1mSv y<sup>-1</sup>) depending on the work activity performed by the artisans, but crushing and sieving Coltan in the mills resulted in the highest dose.

In Kenya, Mangala, 1987 conducted a multi-elemental X-ray fluorescence analysis of soil and rocks samples from the Mrima hills. Thorium, niobium, lead, strontium and zinc were found to be at high concentration in the soil and rock samples. Thorium and traces of rare earth metals were also found in high concentrations (>1000μg/g). The survey by Patel in 1991 indicated that Mrima hills area is composed of deeply weathered carbonitite rocks and has high natural background radioactivity (Patel, 1991). The upper and lower levels of external gamma radiation doses were 106.7mSv and 1.372mSv respectively. Testing of Water samples from some public wells in Mrima showed radon activity levels to be around 100kBqm<sup>-3</sup> (Mustapha, 1999). This was attributed to occurrences of thorium enriched carbonates in the area.

Achola, 2009 carried out a radiological survey in various parts of Lambwe east location (South western Kenya) whose results indicated that the mean estimated annual external effective dose rate due to radionuclides in rocks and soils were 5704.78μSvyr<sup>-1</sup>. The average specific activity concentrations of  $^{40}\text{K}$ ,  $^{226}\text{Ra}$  (uranium-238 equivalent) and  $^{232}\text{Th}$  in rock and soil samples from these areas were measured and found to be 508.67 BqKg<sup>-1</sup>, 178.69 Bq Kg<sup>-1</sup> and 1396.85 BqKg<sup>-1</sup> respectively. The study indicated that the source of enhanced level of natural radioactivity in the sample was mainly carbonatite rocks. Based on the higher levels of gamma-absorbed dose rates in air (5.705mSv/yr) as compared to the global mean of 0.46mSv/yr, this region was considered as high natural background radiation area (HBRA).

Odumo, (2009) carried out a radiological study in the artisanal gold mining belt of southern Nyanza (KENYA). The level of radioactivity in the ore and sediments were found to be below the global average level. Mine waters examined contained low levels of  $^{226}\text{Ra}$  and do not pose any significant radiological problem. The dust loading at the crushing sites was relatively high. The absorbed dose in air due to gamma – ray emitters in the mines was found to be lower than the world average outdoor exposure value of  $55\text{nGy/h}$ . The annual effective dose in the mines is below  $1\text{mSvyr}^{-1}$  and  $20\text{mSvy}^{-1}$ , the limits for the general public and radiation worker respectively.

## 2.2 Limestone Mining and Radiation Exposure

Studies on radioactive elements associated with limestone in most parts of the world have shown low levels of natural radioactivity. However some basement rocks found within limestone deposits may contain slightly elevated levels of  $^{238}\text{U}$ . Mine tailings may therefore contain higher levels of background radioactivity as compared to the limestone.

In Parana basin Southeastern Brazil in an open pit mine, that exploited limestone for production of soil correction compounds and raw materials for ceramic industry, the radioactivity of the sediments was investigated. (Carlos *et al*, 2004). It was reported that the activity concentrations of the main natural radioactive elements;  $^{238}\text{U}$ ,  $^{232}\text{Th}$  and  $^{40}\text{K}$  were generally low with  $^{238}\text{U}$  being enriched in some limestone and shale levels

Wollenberg and Smith, conducted a research on Portland cement in U.S.A. Raw materials from the operating cement plants in California and finished products from over 80 plants in the United States and Canada were subjected to gamma spectrographic evaluation. (Wollenberg and Smith, 2008). The results indicated that limestone, the principal ingredient of cement is low in radioactivity. Uranium was the principal contributor of gamma radioactivity in limestone while thorium was the principal contributor in cement plant shale.

An investigation of radon levels in the caves of Creswell Crags, Derbyshire, in U.K showed that the lower magnesian Limestone (Permian) caves have moderate to raised radon gas levels

(Gillmore et al 2002) which generally increased with increasing distance into the caves from the entrance regions. This feature is partly explained in terms of cave ventilation and topography. While these levels are generally below the action level in the workplace ( $400\text{Bq m}^{-3}$  in the UK), they are above the action level for domestic properties ( $200\text{ Bq m}^{-3}$ ). Creswell Crags has approximately 40,000 visitors per year and therefore a quantification of effective dose is important for both visitors and guides to the Robin Hood show cave. Due to short exposure times the dose received by visitors is low ( $0.0016\text{mSv}/\text{visit}$ ) and regulations concerning exposure are not contravened. Similarly, the dose received by guides is fairly low ( $0.4\text{mSv}/\text{yr}$ ) due in part to current working practice. However, the risk to researchers entering the more inaccessible areas of the cave system is higher ( $0.06\text{mSv}/\text{visit}$ ). This survey also investigated the effect of seasonal variations on recorded radon concentration. From this work summer to winter ratios of between 1.1 and 9.51 were determined for different locations within the largest cave system.

Determination of the radium equivalent, external hazard index, gamma activity index and alpha index calculated from the activity concentrations of  $^{226}\text{Ra}$ ,  $^{232}\text{Th}$  and  $^{40}\text{K}$  obtained from seven brands of Portland cement used in Nigeria indicated that the values were all within the recommended limits for safety in use as building materials (Ademola, 2008).

In Uganda a study of the geology of Kilembe copper-cobalt mine in western Uganda and the Sukulu carbonatite complex in eastern Uganda showed variation of concentrations of radionuclides uranium, thorium and radon gas with the variation in the types of the underlying rocks (Kisolo and Barifaijo, 2008). The radiation exposure levels in Kilembe copper-cobalt mines and the Sukulu limestone had exposure levels ranging from  $0.24\text{ mSv}/\text{y}$  to  $34\text{ mSv}/\text{y}$  which in some cases exceeded the dose limits for both public and workers. The researchers reported possible radiological risks to miners and the members of the public.

Although limestone is widely mined in Kenya for manufacture of cement, no research has been carried out to determine their radioactivity levels. This raises a lot of concern as to the potential risks of exposure especially to the industrial workers and the people living within the vicinity of the cement plants, thus the need for this research.



### 2.3 Mineral Mining and Heavy Metals

Mineral ores are always found mixed with other chemical compounds by nature. Some of these elements are useful to the human body at small quantities but highly toxic at elevated levels. Mining of minerals results to the exposure of these heavy elements to the top soil thus making them readily available for assimilation by plants and consequently consumed by animals and humans. Some oxides of these metals are soluble hence they can easily enter into water bodies thus being easily distributed to other region other than the mining site.

Gregory in 1992 found that the chemical composition of the Columbite grains from Yinnietharra (Western Australia) was (2.2-4.8 wt %) and  $UO_2$  (0.2-2.6 wt %). In addition to  $TiO_2$  and  $UO_2$ , analysis revealed the presence of minor amounts of  $SnO_2$  (0.4-0.8 wt %),  $Y_2O_3$  (0.4-1.4 wt %),  $Ce_2O_3$  (0.3-0.9 wt %), and  $PbO$  (0.0-0.4 wt %). Ti, Y, and U were heterogeneously distributed within the samples.

A study of the concentration of heavy metals from some three old Pb and Zn mine sites in a semi arid zone in south east Spain indicated high total metal concentrations; 5000-8000  $\mu\text{g/g}$  for Pb, 7600-12300  $\mu\text{g/g}$  for Zn (Conesa *et al*, 2006). Two of the mine tailing deposits had a normal soil pH (6-7) while the third was highly acidic with a pH value of 2.5.

A historic input of the mine tailings in the coastal region of Marinduque Island Philippines was traced through variations in heavy metal concentrations (David, 2003). Baseline metal concentrations in porites were established using coral from a reef that was least exposed to contamination. The lowest mean values of Cu (0.7  $\mu\text{g/g}$ ), Mn (0.8  $\mu\text{g/g}$ ) and Zn (1.0  $\mu\text{g/g}$ ) were calculated from annual skeletal bands representing five years of growth. Conversely, a sample of a reef adjacent to an old tailing stock pile displayed consistently elevated values in its growth bands. The mean Cu, Mn and Zn values for this coral were found to be 3.1, 1.0 and 1.8  $\mu\text{g/g}$  respectively. Corals from Ihatub reef showed distinct metal concentration peak in their 1996 growth ring. These peaks coincide with a documented release of mine tailings in the Ihatub area during that year.

Studies on limestone mining and heavy toxic elements have also been done. Prasad and Bose (2001) did a study on six heavy metals: copper, zinc, cadmium, iron, chromium and lead in nine

spring and eight surface water sampling sites near a limestone mining area of Sirmour district of Himachal Pradesh India. The results showed concentrations that were below the permissible levels of drinking water standards. The heavy metal pollution index calculated from the data was far below the index limit of 100 despite the prolific growth of limestone mining in the region (Prasad and Bose, 2001).

## CHAPTER THREE

### THEORETICAL BACKGROUND

#### 3.0 Introduction

This chapter discusses the theoretical background of the analytical techniques used in the study. Hyper Pure Germanium (HPGe) detector spectroscopy for radioactivity measurements as well as Energy Dispersive X-ray Fluorescence (EDXRF) technique for the determination of elemental concentrations in soil and limestone samples. The chapter further highlights the procedures used for the measurement of activity concentrations of the radionuclides and the calculation of the absorbed and the effective dose rates from activity concentrations of radionuclides and measurement of effective dose rates in air and calculation of absorbed dose rates.

#### 3.1 Energy Dispersive X-Ray Fluorescence (EDXRF) Analysis

This is an important technique in the elemental analysis of a multi elemental sample matrix. In X-ray fluorescence analysis, the intensities of the characteristic radiation emitted by the sample after uniform irradiation by a monochromatic X-ray beam are the basis of elemental quantitative analysis. The energy spectrum consists of the characteristic x-rays lines and background contributions due to coherent and incoherent scatterings; the latter tend to interfere with quantitative analysis.

According to Sherman 1955, the dependence of the intensity of fluorescence radiation of element  $i$  and its mass per unit area is given by;

$$I_i(E_i) = G_o K_i \varepsilon(E_i) \cdot \rho_i d_i \left[ \frac{1 - \exp(-a\rho d)}{a\rho d} \right] \dots\dots\dots 3.1$$

Where

$I_i(E_i)$  is the measured fluorescent intensity of element  $i$  in counts per second

$G_o$  is the geometry constant which is also dependent on the source activity as is the case with radioisotope sources.

$K_i$  is the "relative" excitation efficiency (KeV)

$\epsilon(E_i)$  is the relative efficiency of the detector for photons of energy E.

$\rho_i d_i$  is the mass per unit area of element i in the sample in g/cm<sup>2</sup>

$d$  is the thickness of the sample and  $\rho$  its density.

$a$  is a constant for the total mass absorption coefficient

The geometry constant  $G_o$  is given by;

$$G_o = \frac{I_o(E_o)\Omega_1\Omega_2}{\sin\theta_1} \dots\dots\dots 3.2$$

Where;

$I_o(E_o)$  is the intensity of primary exciting radiation (counts/second)

$\Omega_1$  is the solid angle of the incident primary radiation as seen by the sample (Radians).

$\Omega_2$  is the solid angle of the emergent secondary radiation as seen by the detector (Radians).

$\theta_1$  is the incident angle of primary radiation with the sample (Radians ).

The relative excitation coefficient  $K_i$  is given by:

$$K_i = \sigma_i^{\rho h}(E_o) \cdot \left(1 - \frac{1}{J_{is}}\right) \cdot \omega_{is} \cdot f_s^i \dots\dots\dots 3.3$$

Where;

$\sigma_i^{\rho h}(E_o)$  is the photoelectric mass absorption coefficient of element i at energy  $E_o$ .

$\omega_{is}$  is the fluorescence yield for element i in shell "s".

$(1 - \frac{1}{f_{is}})$  is the relative probability for photoelectric effect in shell "s".

$f_s^i$  is the ratio of the intensity of a given K or L line to the intensity of the whole series.

$$a = \mu(E_o)Csc\phi_1 + \mu(E_1)Csc\phi_2, \dots\dots\dots 3.4$$

in which

$\mu(E_o)$  and  $\mu(E_1)$  are the total mass absorption coefficients in the sample at primary and secondary energies.

$\phi_1$ , is the incident angle of primary radiation with the sample.

$\phi_2$ , is the emergent angle of secondary radiation with the sample.

The equation above is derived with the following assumptions being taken into account;

- 1) The excitation source is considered to be a point source.
- 2) The sample is homogeneous.
- 3) The primary radiation is monochromatic.
- 4) The density of element  $i$ ,  $\rho_i$  in the sample is constant over the whole sample volume.
- 5) A fixed geometry is maintained during the intensity measurements of element  $i$  in the sample, thus  $\phi_1$  and  $\phi_2$  are constant and the detector is far from the sample.

The expression  $\left[ \frac{1 - \exp(-apd)}{apd} \right]$  in equation 3.1 is called the absorption correction factor and it accounts for the attenuation of the primary and secondary radiation in the sample.

For thin samples, approximation on the exponential term,

$\exp(-apd) \approx 1 - apd$ , with a relative error of 1% for  $apd \ll 0.01$  is assumed. Thus, equation 3.1 reduces to:

$$I_i(E_i) = G_o \cdot K_i \varepsilon(E_i) \cdot \rho_i d_i \dots\dots\dots 3.5$$

in which  $\rho_i d_i \leq \frac{0.134}{apd}$ . In this case the concentration in terms of the mass per unit area of element  $i$ , is linearly dependent on the fluorescence radiation intensity.

For thick samples, approximation to  $\exp(-apd)$  in equation (3.1), asymptotically tends to zero, for  $apd \gg 1$  Thus, equation (3.1) reduces to;

$$I_i = \frac{G_o.K_i\varepsilon(E_i).\rho_i d_i}{apd} \dots\dots\dots 3.6$$

in which  $\exp(-apd) < 0.01$  where  $\rho_i d_i \geq \frac{0.461}{apd}$  with relative error of 1%. Where all the parameters have same meaning as in equation 3.1

**3.1.1 Matrix Effects**

Matrix effects in EDXRF consist of the influence of variations of chemical composition of the sample on the fluorescence radiation intensity of the wanted element. They constitute the major sources of errors in the method (Mangala, 1987).

There are two types of matrix effects viz;

- 1) Absorption effect, which occurs when the variations in the matrix chemical composition result in changes of the mean absorption of the sample coefficients for both primary radiation and fluorescent radiation of the wanted element. Influence of these variations on  $\mu_i(E_o)$  and  $\mu_i(E_i)$  are evident from the intensity equation 3.1, in which for fixed measurement conditions, the fluorescent radiation is a function of three variables;

$$I_i(E_i) = f[\rho_i d_i, \mu_i(E_o), \mu_i(E_i)] \dots\dots\dots 3.7$$

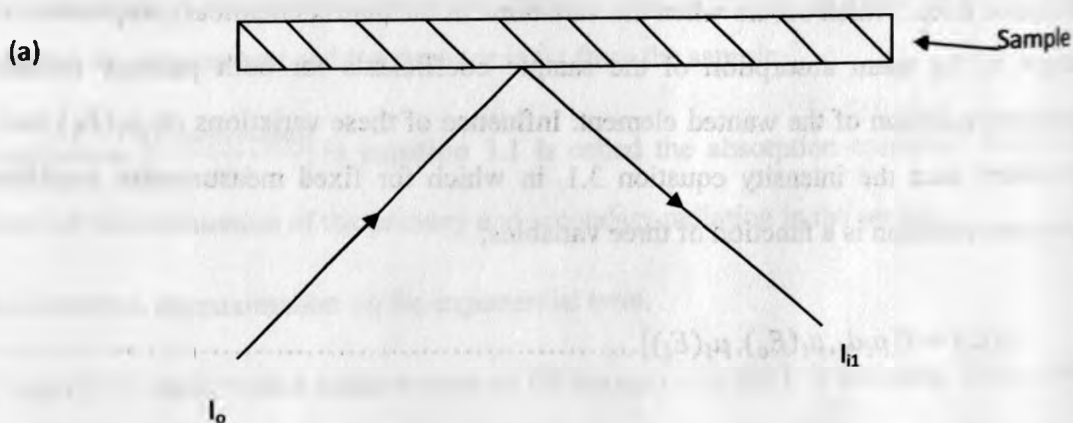
Where all the variables retain the meaning explained under equation 3.1

- 2) Enhancement effect, which consists of additional excitation of the atoms of the wanted element by the fluorescence radiation of the inter-elements. These effects constitute an ensemble of cascade processes in which each one of them consists of excitation of the higher atoms by the fluorescence radiation of the heavier atoms. The intensity of the wanted elements will depend on

the atomic numbers and the concentrations of heavier elements in the sample. Most matrix correction methods have been developed for absorption effects since they are severe. Enhancement effects are minimal especially when analyzing thin and diluted transparent samples of the order of  $\mu\text{g}/\text{cm}^2$  or few hundreds of  $\text{mg}/\text{cm}^2$  for most elements.

### 3.1.2 Matrix Correction Method for Transparent Sample Analysis.

Matrix absorption effects can be experimentally determined for uniform transparent samples. The matrix effects due to absorption are more than enhancement effects. For this reason enhanced effects are considered negligible. The absorption effects are determined by a technique that involves transmission measurements of x-ray intensities from a multi-element target located at a position adjacent to the back of the sample, with and without the sample of known mass per unit area as shown in figure 3.1, (Mangala 1987).



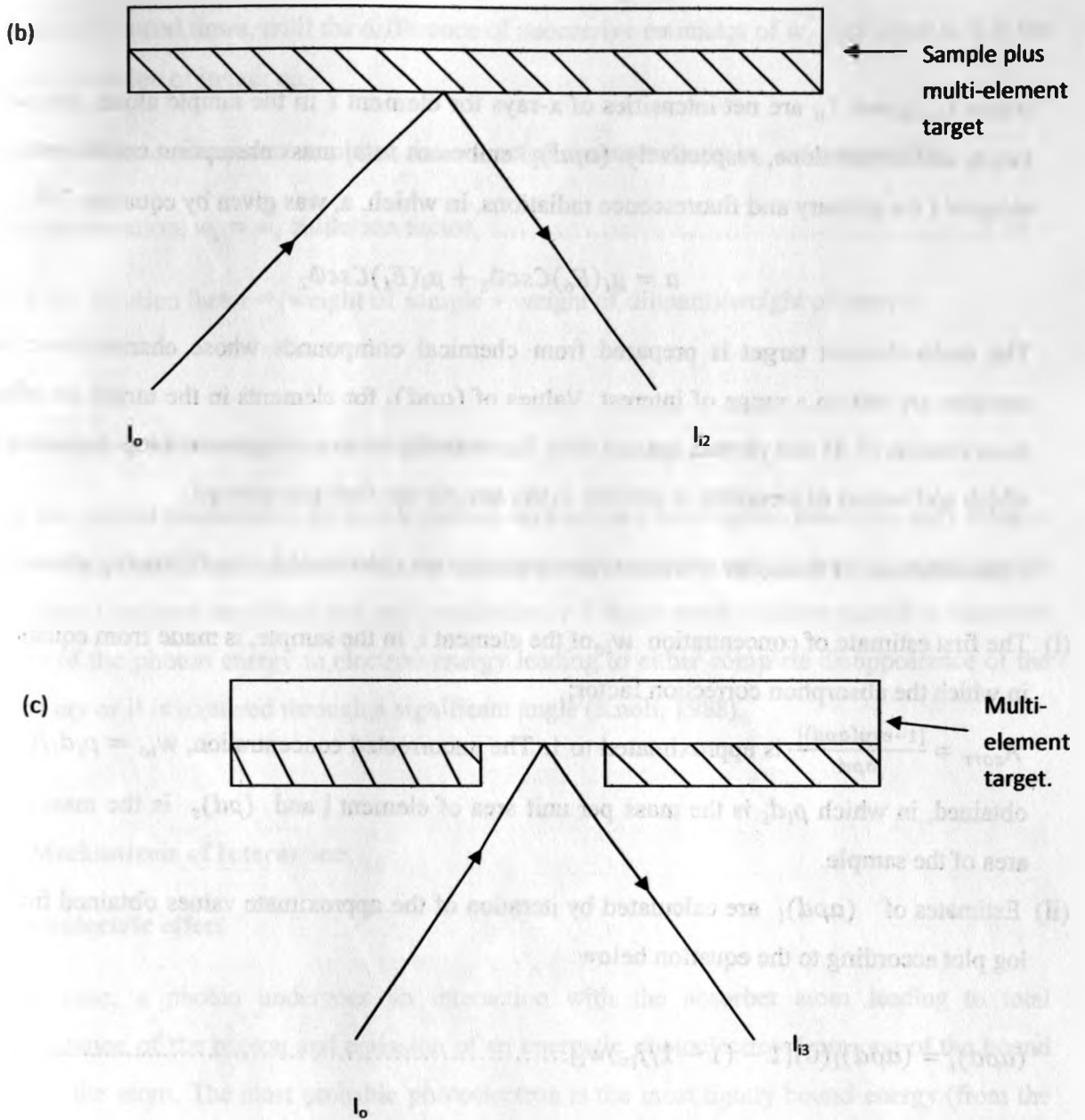


Fig.3.1: Experimental procedure for matrix absorption correction.

The correction factor  $(apd)_i$  for element  $i$  due to absorption of primary and fluorescence radiations transmitted through sample of thickness  $\rho d(g/cm^2)$ , according to Muriithi, A.K (1982), from the attenuation laws, is given by:



$$(apd)_i = \log_e \left( \frac{I_{oi}}{I_{2i} - I_{1i}} \right) \dots \dots \dots 3.8$$

where  $I_{1i}$ ,  $I_{2i}$  and  $I_{oi}$  are net intensities of x-rays for element  $i$  in the sample alone, sample with target, and target alone, respectively  $(apd)_i$  embraces total mass absorption coefficients of the element  $i$  for primary and fluorescence radiations, in which,  $a$ , was given by equation 3.4 i.e

$$a = \mu_i(E_o)Csc\phi_1 + \mu_i(E_i)Csc\phi_2$$

The multi-element target is prepared from chemical compounds whose characteristic x-rays energies are within a range of interest. Values of  $(apd)_i$  for elements in the target are obtained from relation (3.8) and plotted against their fluorescence x-rays energies on a log-log scale, from which  $apd$  values of elements of interest in the sample are then interpolated.

Concentrations of elements of interest in the sample are calculated by the following procedure;

- (i) The first estimate of concentration  $w_{io}$  of the element  $i$ , in the sample, is made from equation 3.2, in which the absorption correction factor;

$A_{corr} = \frac{[1 - \exp(-apd)]}{apd}$  is approximated to 1. The uncorrected concentration,  $w_{io} = \rho_i d_i / (\rho d)_s$  is obtained, in which  $\rho_i d_i$  is the mass per unit area of element  $i$  and  $(\rho d)_s$  is the mass per unit area of the sample.

- (ii) Estimates of  $(apd)_i$  are calculated by iteration of the approximate values obtained from log-log plot according to the equation below:

$$(apd)'_i = (apd)_i(0) [1 - (1 - 1/J_{is})w_i] \dots \dots \dots 3.9$$

in which  $(apd)_i(0)$  value is obtained from the presented curves on log-log scale.,  $(1 - 1/J_{is})$  is the relative probability for photoelectric effect in shell "s".

- (iii)  $(apd)'_i$  from (ii) is in turn used to generate  $A_{corr}$  factor.

(iv) The new concentration estimate,  $w_i' = \frac{w_{io}}{A_{corr}}$ , are substituted in equation 3.4. Steps (ii) and (iii) are repeated several times, until the difference of successive estimates of  $w_i'$  converges to less the required precision of iterations.

In cases of diluted transparent samples, the corrected concentrations  $w_i$  calculated from;

Final concentration,  $w_i = w_i' \times \text{dilution factor} \dots\dots\dots 3.10$

Where the, dilution factor = (weight of sample + weight of dilutant)/weight of sample.

**3.2 Interaction of Gamma Rays with Matter**

There are several mechanisms by which gamma rays interact with matter. However, only three of these methods play an important role in radiation measurement and dosimetry: photoelectric absorption, Compton scattering and pair production. All these result to either partial or complete transfer of the photon energy to electron energy leading to either complete disappearance of the gamma ray or it is scattered through a significant angle (Knoll, 1988).

**3.2.1 Mechanisms of Interaction**

**1. Photoelectric effect**

In this case, a photon undergoes an interaction with the absorber atom leading to total disappearance of the photon and emission of an energetic photoelectron from one of the bound shells of the atom. The most probable photoelectron is the most tightly bound energy (from the K-shell). The energy of the ejected photoelectron is given by the equation;

$$E_e = h\nu - E_b \dots\dots\dots 3.11$$

Where  $E_b$  is the binding energy of the electron in the original shell and  $E_e$  is the energy of the emitted photon. It is most predominant mode of interaction for gamma or X-rays of relatively low energy interacting with materials of high atomic numbers.

## 2. Compton scattering

This takes place between the incident gamma ray photon and electron in the absorbing material. It is the most often predominant mode of interaction for gamma ray energies typical of radioisotopes. In this case the incoming gamma ray is deflected through an angle  $\theta$  from the original direction. The photon transfers a portion of its energy to the electron which is assumed to be at rest. The electron then recoils at angle  $\phi$  with respect to the original direction of photon.

The energy of the scattered photon is given by;

$$h\nu' = \frac{h\nu}{1 + \frac{h\nu}{m_0c^2}(1 - \cos\theta)} \dots\dots\dots 3.12$$

Where  $m_0c^2$  is the rest mass energy of the electron and is equal to 0.511 MeV.

## 3. Pair production

This occurs if the gamma ray energy exceeds twice the rest mass energy of an electron ( $>1.02\text{MeV}$ ). The probability of the interaction remains low until the energy of the photon approaches several MeV thus it's confined to high energy gamma rays. The interaction takes place within the Coulomb field of the nucleus. The photon completely disappears and it is replaced by an electron-positron pair. Since the creation of an electron-positron pair requires only 1.02 MeV of energy the rest of the photon energy is converted to kinetic energy shared by the electron and the positron. The electron and the positron consequently annihilate due to their interaction with the absorbing material leading to production of two annihilation photons as secondary products of the interaction.

### 3.3 Absorbed Gamma Dose Rates in Air, Activity Concentrations and Annual Effective Dose Rates

The exposure to ionizing radiation from natural sources is a continuous and un-avoidable feature of life on earth. The major sources responsible for this exposure are the presence of naturally occurring radionuclides in the earth's crust. Effective dose rates are measured using gamma ray survey meters at 1m height above the ground which represents the standard height of human sensitive body organs (UNSCEAR, 1993). The absorbed gamma dose rates in air at 1m above the ground surface for the uniform distribution of radionuclides are computed on the basis of guidelines provided by UNSCEAR (1993, 2000). Absorbed dose rates in air in  $\text{nGy h}^{-1}$  are computed from the dose rates in  $\mu\text{Sv h}^{-1}$  as measured in the field using the conversion coefficient factor of  $0.7\text{Sv Gy}^{-1}$  as stated by UNSCEAR, 2000. Alternatively, absorbed dose rates,  $D$  ( $\text{nGy h}^{-1}$ ) in air at about 1m above ground can also be calculated from the activity concentrations of  $^{232}\text{Th}$ ,  $^{238}\text{U}$  equivalent and  $^{40}\text{K}$ . Conversion factors used to compute absorbed gamma dose rate ( $D$ ) in air per unit activity concentration ( $\text{Bq Kg}^{-1}$ ) in geological samples are given in UNSCEAR, 2000. For instance, sand corresponds to  $0.621\text{nGy h}^{-1}$ , for  $^{232}\text{Th}$ ,  $0.462\text{nGy h}^{-1}$  for  $^{238}\text{U}$ , and  $0.0417\text{nGy h}^{-1}$  for  $^{40}\text{K}$ .

Based on the measured gamma-ray photo-peak intensities, emitted by specific radionuclides in the  $^{232}\text{Th}$  and  $^{238}\text{U}$  equivalent decay series and in  $^{40}\text{K}$ , their activity concentrations in the samples are determined. Calculations rely on the establishment of secular equilibrium in the samples, due to the much smaller lifetime of daughter nuclides in the decay series of  $^{232}\text{Th}$  and  $^{226}\text{Ra}$  (Mohanty et al, 2004). More specifically, the  $^{232}\text{Th}$  activity concentration is determined from the concentrations of  $^{212}\text{Pb}$  in the samples, and that of  $^{238}\text{U}$  equivalent is determined from the average concentrations of the  $^{214}\text{Pb}$  decay products. Thus, an accurate measurement of  $^{232}\text{Th}$  and  $^{238}\text{U}$  equivalent activity concentrations is made, whereas a true measurement of  $^{40}\text{K}$  concentration is achieved. The well known interference between the gamma lines of  $^{226}\text{Ra}$  (186.20 keV) and  $^{235}\text{U}$  (185.7 keV) is inevitable, especially in the presence of a relatively high uranium concentration and, therefore, the above mentioned line is not used for the determination of the activity concentration of  $^{238}\text{U}$  equivalent (Mohanty et al, 2004).

The detector is energy calibrated using a standard source (SRM -1) supplied by the international energy atomic agency (IAEA). Certified reference materials i.e. RGU-1, RGTh-1, and RGK-1,

which are produced under the auspices of the IAEA and distributed through its Analytical Quality Control Services (AQCS) program, are sealed in the same beakers as the samples and measured for reasonable number of hours each. The results obtained from the samples and certified reference materials are substituted in the comparison method formula to get activity concentrations of the primordial radionuclides. Either the comparison formula method or absolute formula method is used for determining activity concentrations. Comparison method incorporates mass of the sample, intensity of the sample, activity of the sample, mass of reference material, intensity of reference material, and activity of reference material. To estimate the annual effective external dose rates, the conversion coefficient of absorbed dose in air to effective dose of  $0.7\text{Sv Gy}^{-1}$  and outdoors occupancy factor (0.2) proposed by UNSCEAR (2000) are used. This occupancy factor value is however, not representative of the area of study. In Europe and other extremely cold countries where a lot of time is spent indoors than outdoors, outdoor occupancy factor is taken as 0.2 (UNSCEAR, 2000) is applied. For this area of study, people tend to stay outdoor for longer time due to friendly climate while attending to their daily duties and an outdoor occupancy factor of 0.4 is applicable (Mustapha, 1999).

## **CHAPTER FOUR**

### **MATERIALS AND METHODS**

#### **4.0 Introduction**

This chapter discusses details of the procedures used for sampling, sample preparation, description of the study area and data analysis.

#### **4.1 Study Area**

The study area was divided into 3 sampling regions that represent the main limestone deposits; region 1 stretches about 10 kms to the east of Kanziku town currently referred to as Utekilawa-Kituvwi Hills, region 2 borders Kanziku town to the west and stretches westwards to a distance of 12 km Katyethoka market and covers Kamaluu and Mwanyani Hills while region 3 lies about 15 km along the main road towards Mutomo town hereby referred to as Ndulukuni Hill, see figure 1 on page 6.

#### **4.2 Sampling**

Twenty soil and 20 limestone samples each weighing approximately 500g were collected randomly from each region and packed into well labeled plastic bags. The sample bags were labeled so as to indicate the region and the sample number and sample type e.g S101 meaning soil sample, from region 1 sample number 01 and L201 meaning limestone sample from region 2, sample number 01. The soil samples were collected at depth range of 0-15cm. Limestone samples were collected from the numerous rock outcrops where possible. However, where limestone ore was not exposed the samples were obtained from the various exploration points drilled by mineral exploration companies.

### 4.3 Energy Dispersive X-Ray Fluorescence Spectrometric Analysis

It consists of solid-state detector Si(Li), pre-amplifier, amplifier, and a multi-channel analyzer (MCA). A microcomputer with a relevant interface is also incorporated. The resultant spectra were collected on the multi-channel analyzer in the pulse height analysis mode, and then stored on magnetic floppy diskettes for quantitative analysis (figure 4.1) The final concentration of an element of interest measured is the mean of the concentration values of measurements three pellets.

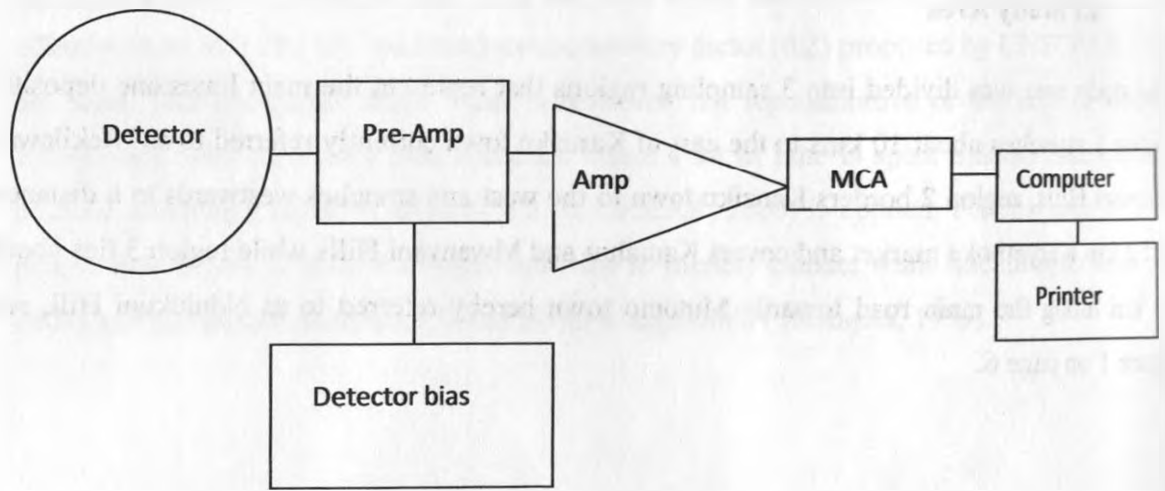


Fig. 4.1: Block diagram of EDXRF spectrometer.

### 4.4 EDXRF Procedures

The soil and limestone samples were dried and pulverized into fine powder before being sieved to obtain a powdered matrix of particle size 75 $\mu$ m. The powdered soil and limestone samples were mixed with 30% and 50% starch by mass respectively for ease of pellet preparation. Three pellets of mass between 0.3-0.5g were prepared from each sample for analysis. Each pellet was irradiated for 1500 seconds using  $^{109}\text{Cd}$  source for heavy metals and  $^{55}\text{Fe}$  for low atomic mass elements and the spectra analyzed using software MCA Canberra S100. A specialized software Axil was used for peak de-convolution and elemental quantitative analysis. Validation of the EDXRF method was done using soil certified reference material CRM SOIL-7 from IAEA

(International Atomic Energy Agency) and the detection limits of individual elements of interest computed.

The average metal concentrations for Ca, Ti, Mn, Fe, Cu, Zn and Pb in both limestone and soil samples were calculated as the average concentration of the three pellets prepared for analysis. These results were then compared with soil metal concentration limits for the calculation of heavy metal pollution index. The concentration of the heavy metals Cu, Zn and Pb were compared with the calcium content in the limestone in order to establish the relationship between the quantity of limestone in ore and the heavy metal contents in the ore. Metal pollution indexes were obtained by dividing the measured metal concentrations in samples by the U.S EPA soil metal concentration limits. For the soil to be considered contaminated with a particular element the metal pollution index should exceed 1 (Sipos and Poka, 2000 )

#### **4.5 Measurement of External Gamma Doses and External Effective Doses in Air.**

The external effective dose rates at 1m above the ground were measured at each sampling point using a Radiation survey meter PKCB – 104, Serial number 910024240 from PKCB Canada. The equipment was calibrated at the Kenya Bureau of Standards and measurements calculated using a calibration factor of 3.64. About 15 readings were taken for each point and the average calculated to determine the effective dose rates in  $\mu\text{Sv/h}$ . The absorbed gamma dose rates in air at 1m above the ground surface for the uniform distribution of radionuclides were computed from the effective dose rates measured at the ground using a conversion coefficient factor of 0.7 Sv/Gy as per the guidelines provided by UNSCEAR (1993, 2000). The absorbed dose rates, D ( $\text{nGy h}^{-1}$ ) in air at about 1m above ground were also calculated from the activity concentrations of  $^{232}\text{Th}$ ,  $^{238}\text{U}$  equivalent and  $^{40}\text{K}$ . Conversion factors used to compute absorbed gamma dose rate (D) in air per unit activity concentration ( $\text{Bq Kg}^{-1}$ ) in geological samples for instance sand corresponds to  $0.621\text{nGy h}^{-1}$ , for  $^{232}\text{Th}$ ,  $0.462\text{nGy h}^{-1}$  for  $^{238}\text{U}$ , and  $0.0417\text{nGy h}^{-1}$  for  $^{40}\text{K}$ .





$^{212}\text{Pb}$  and  $^{228}\text{Ac}$  in the samples, and that of  $^{238}\text{U}$  equivalent was determined from the average concentrations of the  $^{214}\text{Pb}$  and  $^{214}\text{Bi}$  decay products. Thus, an accurate measurement of  $^{232}\text{Th}$  and  $^{238}\text{U}$  equivalent activity concentrations is made, whereas a true measurement of  $^{40}\text{K}$  concentration is achieved.

To estimate the annual effective external dose rates, the conversion coefficient from absorbed dose in air to effective dose ( $0.7\text{Sv Gy}^{-1}$ ) was used. However, the outdoor occupancy factor (0.2) proposed by UNSCEAR (2000) could not be used taking in to account the friendly climate in this region that makes people spend more time outdoors. An occupancy factor of 0.4 was thus applied as suggested by Mustapha (1999).

#### **4.7 Gamma Ray Spectrometry**

Measurement of activity concentrations of the naturally occurring radionuclides in pulverized limestone ore samples was performed with high-purity germanium (HPGe) gamma-ray detector with 144cc as the active volume and outside diameter of 76mm. The detector has an efficiency of 31.6% and a resolution of 1.8keV. Each sample was put into a detector shielded with a thick walled hollow lead cylinder and measured for between 12 hours or more depending on the samples activity. Prior to the samples measurement, the environmental gamma background inside the laboratory was determined using a similar plastic container filled with double distilled water under identical measurement conditions and subtracted from the measured gamma ray spectra of each sample. Each measured gamma-ray spectrum was analyzed off line by a dedicated software program PCA3. (See figure 4.2)

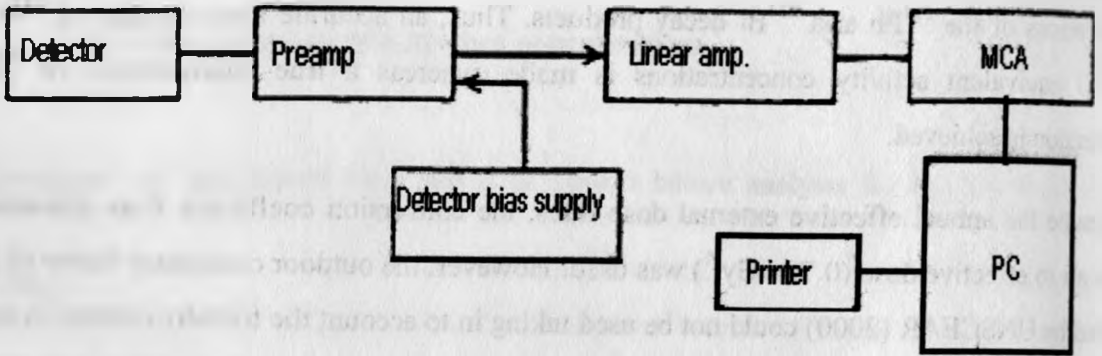


Fig.4.2:Block diagram of hyper pure germanium spectrometer.

## CHAPTER FIVE

### RESULTS AND DISCUSSION

#### 5.0 Introduction

This chapter discusses results of all the measurements obtained in this study. Quantitative analysis of soil metal content and calculation of their pollution indexes are also presented. The activity concentrations, absorbed gamma dose rates and annual effective dose rates were calculated from the activity concentrations of radionuclides. The measured effective dose rates were compared with the ones obtained from activity concentrations. The results are discussed in relation to similar related studies in other parts of the world.

#### 5.1 Elemental Analysis

##### 5.1.1 Region 1(Utekilawa-Kituvwi Hills)

###### Soils

The concentration of Cu in soil samples analysed from Utekilawa – Kituvwi Hills was mainly below the detection limits except for only 1 sample whose concentration was  $49.6 \mu\text{g/g} \pm 16$ . The calculated Cu soil pollution index was 0.66. This indicates that the soils in this region were not contaminated with copper.

Zn was found in almost all the samples analysed with average concentration was found to be  $79.8 \mu\text{g/g} \pm 27$ . The values ranged from  $33.3 \mu\text{g/g} \pm 8$  to  $103 \mu\text{g/g} \pm 11$ . The pollution indexes were found to range from 0.168 to 0.516 with a mean Zn pollution index was  $0.384 \pm 0.13$ .

Lead metal was found in 2 samples. The values were  $31.7 \mu\text{g/g} \pm 10$  and  $27.9 \mu\text{g/g} \pm 8$ . Pollution indexes were thus found to be 0.317 and 0.28 respectively. In general the results indicate that the soils in this region were not contaminated with heavy metals Cu, Zn and Pb (see table 5.1 and 5.2).

**Table 5.1: Metal concentration for soil samples from Utekilwa-Kituvwi Hills**

SAMPLE CODE	Ca	Ti	Mn	Fe	Cu	Zn	Pb
S101	46122±2890	6372±551	1540±126	61451±3010	<7	86.8±14	<3
S102	19395±1655	4719±445	680±80	33392±1650	<7	<8	<3
S103	12477±1285	4799±413	550±67	26660±1315	<7	71.8±10	<3
S104	15063±1475	5152±458	583±76	36791±1810	<7	65.9±11	<3
S105	12277±1325	4399±413	422±64	22261±1102	<7	33.5±9	<3
S106	17262±1565	5798±485	953±9	40990±2015	<7	77.4±12	<3
S107	14796±1475	5692±476	720±81	39523±1945	<7	98.7±12	<3
S108	19795±2070	7651±675	806±109	37657±1855	<7	43.1±14	<3
S109	16795±1565	9084±638	1312±111	65784±3235	<7	134.0±16	<3
S110	27460±1950	8478±602	1124±102	54520±2675	<7	82.8±14	<3
S111	15663±1430	8918±606	847±90	77247±3775	<7	<8	<3
S112	61118±2170	8505±601	920±93	65850±3220	49.6±15	<8	<3
S113	59785±3450	5978±523	911±91	42456±2090	<7	75.6±12	<3
S114	17666±1505	5666±471	1029±94	43552±2135	<7	91.5±12	<3
S115	18728±1655	4912±449	661±80	27726±1370	<7	41.6±10	<3
S116	19995±1720	6218±529	944±96	82579±2415	<7	85.8±13	<3
S117	24260±1730	4266±387	982±84	26660±1320	<7	103.2±11	27.9±8
S118	18129±1530	5272±444	814±81	40657±1995	<7	70.7±12	<3
S119	19528±2070	7651±675	806±109	37657±1855	<7	90.4±14	<3
S120	20528±1780	6745±554	872±94	52787±2590	<7	31.7±10	<3

**Table 5.2 Heavy Metal Pollution Indexes for Soils from Utekilawa-Kituvwi Hills**

Sample	Copper		Zinc		Lead	
	Conc. (µg/g)	Pollution index	Conc. (µg/g)	Pollution index	Conc. (µg/g)	pollution Index
S101	<7	-	86.8±14	0.43	<3	-
S102	<7	-	<8	-	<3	-
S103	<7	-	71.8±10	0.36	<3	-
S104	<7	-	65.9±11	0.33	<3	-
S105	<7	-	33.5±9	0.17	<3	-
S106	<7	-	77.4±12	0.39	<3	-
S107	<7	-	98.7±12	0.49	<3	-
S108	<7	-	43.1±14	0.22	<3	-
S109	<7	-	134.0±16	0.67	<3	-
S110	<7	-	82.8±14	0.41	<3	-
S111	<7	-	<8	-	<3	-
S112	49.6±15	-	<8	-	<3	-
S113	<7	-	75.6±12	0.38	<3	-
S114	<7	0.66	91.5±12	0.46	<3	-
S115	<7	-	41.6±10	0.21	<3	-
S116	<7	-	85.8±13	0.43	<3	-
S117	<7	-	103.2±11	0.52	27.9±8	0.28
S118	<7	-	70.7±12	0.35	<3	-
S119	<7	-	90.4±14	0.45	<3	-
S120	<7	-	31.7±10	0.16	<3	-

## Limestone

The Cu concentrations were found to be below the detection limits for all the limestone samples analysed except 1 where the concentration of Cu was found to be as high as  $187.5 \mu\text{g/g} \pm 18$  giving pollution index of 2.50 which signifies a high level of contamination. The Ca content for this sample was low ( $< 10\%$ ) by mass when compared to the mean Ca content for rest of the samples from the region. This high concentration could thus be attributed to weathering and other geochemical processes of other rocks rather than the limestone ore. (Bárány *et al*, 1991). These results also agree with other study results in Hungary which indicated higher heavy metal content in karst soils than it should be, if it originated from the parent rock alone (Keveiné-Bárány *et al* 1999).

Zn was found to be below the detection limits in all the limestone samples. A comparison with soil samples from the same region in which Zn concentrations were at significantly high levels in all the samples gives an indication that the zinc present in the soil samples is not associated to limestone ore. These sources are likely to be the rocks underlying the limestone deposits in the area which include graphite bands and marbles whose outcrops consist principally of calcite crystals (Saggerson, 1957).

Lead concentrations for most samples were below detection limits except in 3 samples only, whose concentrations ranged from  $20.7 \mu\text{g/g} \pm 5$  to  $35.4 \mu\text{g/g} \pm 6$  with a mean value of  $26.7 \mu\text{g/g} \pm 8$ . The lead pollution indexes were found to range from 0.21 to 0.35 with a mean value of 0.27 and a standard deviation of 0.08. These levels had no significant difference with lead levels in soil samples indicating no contamination with lead. These results were found to be similar to the observations made in a study of the metal content of limestone in Hungary and England (Kabata-Pendias and Pendias, 1984). The heavy metal concentrations for limestone samples and their metal pollution indexes are presented in tables 5.3 and 5.4.

**Table 5.3: Metal Concentration for Limestone Samples from Utekilwa-Kituvwi Hills**

SAMPLE CODE	Ca	Ti	Mn	Fe	Cu	Zn	Pb
L101	346500±15700	<500	<99	462±68	<7	<8	<3
L102	303000±13700	<500	<99	621±67	<7	<8	<3
L103	258000±11800	<500	<99	3870±199	<7	<8	<3
L104	222000±10400	<500	<99	456±49	<7	<8	<3
L105	331500±14700	<500	<99	476±48	<7	<8	<3
L106	298500±13600	<500	<99	832±77	<7	<8	<3
L107	291000±13200	<500	279±73	417±54	<7	<8	<3
L108	291750±13300	<500	<99	942±80	<7	<8	<3
L109	252750±11415	<500	<99	983±73	<7	<8	<3
L110	334500±15200	<500	<99	1476±107	<7	<8	35.4±6
L111	237000±11000	<500	308±68	621±61	<7	<8	20.7±5
L112	430500±19700	<500	<99	2505±161	<7	<8	<3
L113	285000±13100	<500	<99	1875±117	<7	<8	24.8±5
L114	351000±16000	<500	<99	870±85	<7	<8	<3
L115	222000±10400	<500	<99	686±62	<7	<8	<3
L116	303750±13800	<500	<99	470±63	<7	<8	<3
L117	243000±11500	<500	<99	422±56	187.5±18	<8	<3
L118	389250±17450	<500	<99	307±59	<7	<8	<3
L119	385500±17400	<500	<99	627±75	<7	<8	<3
L120	384750±17200	<500	<99	2183±140	<7	<8	<3



**Table 5.4 Limestone Pollution Indexes for Soils from Utekilawa-Kituvwi Hills**

Sample	Copper		Zinc		Lead	
	Conc. (µg/g)	Pollution index	Conc. (µg/g)	Pollution index	Conc. (µg/g)	pollution Index
L101	<7	-	<8	-	<3	-
L102	<7	-	<8	-	<3	-
L103	<7	-	<8	-	<3	-
L104	<7	-	<8	-	<3	-
L105	<7	-	<8	-	<3	-
L106	<7	-	<8	-	<3	-
L107	<7	-	<8	-	<3	-
L108	<7	-	<8	-	<3	-
L109	<7	-	<8	-	<3	-
L110	<7	-	<8	-	35.4±6	0.35
L111	<7	-	<8	-	20.7±5	0.21
L112	<7	-	<8	-	<3	-
L113	<7	-	<8	-	24.8±5	0.25
L114	<7	-	<8	-	<3	-
L115	<7	-	<8	-	<3	-
L116	<7	-	<8	-	<3	-
L117	187.5±18	2.50	<8	-	<3	-
L118	<7	-	<8	-	<3	-
L119	<7	-	<8	-	<3	-
L120	<7	-	<8	-	<3	-

## 5.1.2 Region 2 (Kamaluu- Mwanyani Hills)

### Soils

In this region 7 of the samples had Cu concentrations above detection limits (Table 5.6). The levels ranged from  $43.2 \mu\text{g/g} \pm 11$  to  $86.2 \mu\text{g/g} \pm 19$  with a mean value of  $65.3 \mu\text{g/g} \pm 16$ . The calculated pollution indexes were mainly below 1 with an average of 0.87 indicating that the Cu metal concentrations were below the maximum recommended soil Cu limits ( $75\mu\text{g/g}$ ). However, two of the samples, showed high pollution index of 1.15 and 1.12 respectively indicating a certain extent of contamination in these two samples.

Zinc concentrations ranged from  $34.4 \mu\text{g/g} \pm 11$  to  $154 \mu\text{g/g} \pm 17$  with a mean value of  $77.7 \mu\text{g/g} \pm 29$ . These values are lower than the United States Environmental Protection Agency (U.S. EPA) soil Zn limits. The pollution indexes ranged from 0.17 to 0.77. The mean pollution index was found to be  $0.39 \pm 0.14$  suggesting that the soils in the region were not contaminated with zinc.

Only six of the samples had lead concentrations above detection limits with values ranging from  $19.9 \mu\text{g/g} \pm 8$  to  $72 \mu\text{g/g} \pm 5$  with an average of  $37.2 \mu\text{g/g} \pm 18$ . The pollution indexes ranged from 0.20 to 0.72 with an average of  $0.37 \pm 0.19$ . The results are presented in table 5.5

**Table 5.5 Metal Concentration for Soil Samples from Kamaluu-Mwanyani Hills**

Sample code	Ca	Ti	Mn	Fe	Cu	Zn	Pb
S201	25336±1915	7541±598	1364±112	56924±2790	86.2±15	154.2±17	<3
S202	18021±1950	4389±395	775±76	46350±2275	<7	95.7±11	72.2±5
S203	20083±1575	10873±1085	982±87	35777±1765	<7	59.4±10	<3
S204	107464±5535	7814±334	822±81	15893±795	<7	60.4±9	19.9±8
S205	45885±2650	2461±314	654±69	18287±907	<7	134.0±12	25.2±8
S206	68694±3755	17290±1022	1135±106	59451±2920	<7	81.8±13	23.1±9
S207	79467±4320	7913±591	1107±101	47082±2315	52.7±16	57.9±11	<3
S208	17755±1460	5180±440	620±71	35178±1735	<7	73.5±11	<3
S209	37306±1230	6165±467	587±72	53200±2605	54.6±14	43.8±11	<3
S210	7986±1090	7614±530	666±75	59650±2920	66.6±9	71.6±11	<3
S211	12954±1405	3870±378	393±62.7	25536±1260	<7	56.8±10	<3
S212	16691±1440	5007±424	755±77	367741±805	<7	76.2±11	<3
S213	19551±1625	5852±493	529±737	28395±1405	<7	64.7±10	<3
S214	17223±1555	3830±389	769±79	34846±1715	<7	90.8±12	<3
S215	24804±1720	7128±521	1723±124	59983±2940	73.9±14	99.8±13	40.0±9
S216	38370±2395	13479±835	2760±178	53862±2695	<7	78.6±13	<3
S217	18952±1970	8212±635	1027±104	64704±3175	84.0±17	60.7±11	<3
S218	19019±1510	5207±434	688±81	35843±1765	43.2±11	72.7±10	43.0±10
S219	42759±2640	6270±487	764±81	48811±2395	78.3±14	83.0±12	<3
S220	11444±1225	7328±519	686±75.7	62443±3060	52.5±12	34.4±11	43.0±9

**Table 5.6 Soil Pollution Indexes for Soils from Kamaluu-Mwanyani Hills**

Sample	Copper		Zinc		Lead	
	Conc. ( $\mu\text{g/g}$ )	Pollution index	Conc. ( $\mu\text{g/g}$ )	Pollution index	Conc. ( $\mu\text{g/g}$ )	pollution Index
S201	86.2 $\pm$ 15	1.15	154.2 $\pm$ 17	0.77	<3	<3
S202	<7	-	95.7 $\pm$ 11	0.48	72 $\pm$ 5	72.2 $\pm$ 5
S203	<7	-	59.4 $\pm$ 10	0.30	<3	<3
S204	<7	-	60.4 $\pm$ 9	0.30	19.9 $\pm$ 8	19.9 $\pm$ 8
S205	<7	-	134.0 $\pm$ 12	0.67	25.2 $\pm$ 8	25.2 $\pm$ 8
S206	<7	-	81.8 $\pm$ 13	0.41	23.1 $\pm$ 9	23.1 $\pm$ 9
S207	52.7 $\pm$ 16	0.71	57.9 $\pm$ 11	0.29	<3	<3
S208	<7	-	73.5 $\pm$ 11	0.37	<3	<3
S209	54.6 $\pm$ 14	0.73	43.8 $\pm$ 11	0.22	<3	<3
S210	66.6 $\pm$ 9	0.89	71.6 $\pm$ 11	0.36	<3	<3
S211	<7	-	56.8 $\pm$ 10	0.29	<3	<3
S212	<7	-	76.2 $\pm$ 11	0.38	<3	<3
S213	<7	-	64.7 $\pm$ 10	0.33	<3	<3
S214	<7	-	90.8 $\pm$ 12	0.46	<3	<3
S215	73.9 $\pm$ 14	-	99.8 $\pm$ 13	0.50	40.0 $\pm$ 9	40.0 $\pm$ 9
S216	<7	-	78.6 $\pm$ 13	0.39	<3	<3
S217	84.0 $\pm$ 17	1.12	60.7 $\pm$ 11	0.31	<3	<3
S218	43.2 $\pm$ 11	-	72.7 $\pm$ 10	0.37	43.0 $\pm$ 10	43.0 $\pm$ 10
S219	78.3 $\pm$ 14	-	83.0 $\pm$ 12	0.42	<3	<3
S220	52.5 $\pm$ 12	-	34.4 $\pm$ 11	0.17	43.0 $\pm$ 9	43.0 $\pm$ 9

### Limestone

Limestone samples were mainly found to contain copper below detection limits except in three samples with concentration levels of 132.0  $\mu\text{g/g}\pm 19$ , 162.0  $\mu\text{g/g}\pm 19$  and 106  $\mu\text{g/g}\pm 14$  with a mean of 133.32  $\mu\text{g/g} \pm 28$ . The pollution indexes were thus above 1 indicating significant levels of pollution i.e 2.16, 1.41 and 1.77 with a mean of 1.78. Limestone being mainly calcium

carbonate, calcium was used to compare the quantity of limestone in the ore and concentration of the heavy metals.

Low calcium (<10% Ca by mass) limestone ores were found to contain more copper than high limestone content ore. It was also noted that for all the samples analysed that had calcium concentration above 10%, copper was always below detection limits but whenever the calcium concentration went below this value significantly higher levels of Cu were detected. This implies that limestone ore contains lower contents of copper than the other rocks and that the copper content of the soil could be attributed to weathering and other geo-chemical processes. This inference is similar to studies done in Hungary and England (Keveiné-Bárány *et al* 1999).

Zinc concentrations were found in 7 (35%) samples with values ranging from  $49.8 \mu\text{g/g} \pm 11$  to  $144 \mu\text{g/g} \pm 16$  and a mean concentration of  $92.6 \mu\text{g/g} \pm 32$ . The calculated pollution indexes were all below 1 ranging from 0.249 to 0.720, with an average of  $0.460 \pm 0.15$ . The correlation between the level of zinc and the quantity of limestone in the limestone ore was determined by comparing Zn and Ca concentrations in the ore. A very weak correlation was noted. However, for all the samples with Ca concentrations that were above 11%, it was found that Zn was always below detection limits. From this it was inferred that the underlying rocks contained more Zn than the limestone itself. These results concur with studies done in Hungary and England (Kabata-Pendias and Pendias, 1984).

Lead was detected in only four samples in which the concentrations ranged from  $26.8 \mu\text{g/g} \pm 6$  to  $42.4 \mu\text{g/g} \pm 10$ . These values were below the soil lead concentration limits of  $100 \mu\text{g/g}$  (Sipos and Poka, 2000). The pollution indexes were found to range from 0.27 - 0.42 with a mean of 0.34. A comparison of Pb and Ca concentrations showed that Pb was more prevalent in low Ca (<10% Ca by mass) concentration ores than in high Ca (>10% Ca by mass) concentration ores as was shown for Cu and Zn. (Tables 5.7 and 5.8)

**Table 5.7: Metal Concentration for Limestone Samples in Kamaluu-Mwanyani Hills**

SAMPLE CODE	Ca	Ti	Mn	Fe	Cu	Zn	Pb
L201	329396±16833	<500	<100	1995±139	<7	<8	<3
L202	292600±14800	2075±540	1095±127	24472±1230	<7	<8	<3
L203	75078±4625	2959±476	1066±121	62310±3065	<7	125.0±18	<3
L204	104538±5863	3325±495	2494±178	40343±1993	<7	73.7±14	<3
L205	110400±5320	1875±331	1312±97	26850±1180	<7	48.1±5	<3
L206	106795±5070	1666±333	1432±104	25343±1079	<7	79.8±11	<3
L207	81618±4627	2467±405	1782±136	43757±2153	132.1±19	144.0±16	42.5± 7
L208	30303±2125	2045±328	255±58	12904±563	<7	<8	40.3±9
L209	51648±3437	<500	<100	2837±62	<7	<8	<3
L210	24075±1765	3120±344	709±81	44175±1930	162.7±19	91.1±12	28.0±6
L211	384500±17433	<500	<100	2575±156	<7	<8	<3
L213	238607±13066	<500	739±102	22128±1200	<7	<8	<3
L214	215280±10800	<500	538±74	2639±154	<7	<8	26.8±6
L215	336750±15300	<500	<100	3352±172	<7	<8	<3
L216	329251±16600	<500	308±85	3505±208	<7	<8	<3
L217	46965±2605	4255±385	925±80	48592±2045	106.0±14	86.7±11	<3

**Table 5.8: Metal pollution indexes for limestone samples from Kamaluu-Mwanyani Hills**

Sample Code	Copper		Zinc		Lead	
	Conc. ( $\mu\text{g/g}$ )	Pollution index	Conc. ( $\mu\text{g/g}$ )	Pollution index	Conc. ( $\mu\text{g/g}$ )	pollution Index
L201	<7	-	<8	-	<3	-
L202	<7	-	<8	-	<3	-
L203	<7	-	125.0 $\pm$ 18	0.63	<3	-
L204	<7	-	73.7 $\pm$ 14	0.37	<3	-
L205	<7	-	48.1 $\pm$ 5	0.24	<3	-
L206	<7	-	79.8 $\pm$ 11	0.40	<3	-
L207	132.1 $\pm$ 19	1.76	144.0 $\pm$ 16	0.77	42.5 $\pm$ 7	0.43
L208	<7	-	<8	-	40.3 $\pm$ 9	0.40
L209	<7	-	<8	-	<3	-
L210	162.7 $\pm$ 19	2.16	91.1 $\pm$ 12	0.46	28.0 $\pm$ 6	0.28
L211	<7	-	<8	-	<3	-
L213	<7	-	<8	-	<3	-
L214	<7	-	<8	-	26.8 $\pm$ 6	0.27
L215	<7	-	<8	-	<3	-
L216	<7	-	<8	-	<3	-
L217	106.0 $\pm$ 14	1.41	86.7 $\pm$ 11	0.44	<3	-
L218	<7	-	<8	-	<3	-

### 5.1.3 Region 3 (Ndulukuni Hills)

Copper was found in only 1 sample with a concentration level of,  $69.7 \mu\text{g/g} \pm 11$  and pollution index of 0.93 which was considered as an outlier. Zinc was detected in 15 (75%) of the samples analysed with concentrations ranging from  $36.8 \mu\text{g/g} \pm 9$  to  $174 \mu\text{g/g} \pm 48$  with a mean value of  $99.3 \mu\text{g/g} \pm 42$ . However, 1 sample had zinc content as high as  $854 \mu\text{g/g} \pm 48$  and was considered as an outlier. The zinc pollution indexes were found to have a mean value of 0.5 with values ranging from 0.18 to 0.87. Lead was found in only 2 whose concentrations were  $45.1 \mu\text{g/g} \pm 9$  and  $44.7 \mu\text{g/g} \pm 9$  all which were considered to be outliers. The soils could thus be said not be contaminated with lead (table 5.9).



**Table 5.9: Metal concentration for Soil samples in Ndulukuni Hills**

Sample code	Ca	Ti	Mn	Fe	Cu	Zn	Pb
S301	91947±4855	3579±402	387±71	32392±1590	<7	<8	<3
S302	6098±955	7491±527	750±76	57119±2795	<7	<8	<3
S303	47588±2875	8051±600	1966±139	48455±2380	<7	75.2±12	<3
S304	20462±1595	6145±481	1130±97	50187±2460	<7	124.0±14	<3
S305	63184±3545	5799±490	2586±169	57119±2800	<7	174.2±17	<3
S306	19329±1690	6558±530	718±84	36324±1785	<7	82.8±12	<3
S307	21795±1605	3145±334	674±70	25194±1240	<7	95.5±11	<3
S308	42923±2620	4532±432	1149±100	46988±2305	<7	143.4±15	<3
S309	53320±3730	9664±861	2186±193	102641±5030	<7	164.9±24	<3
S310	75848±4170	6972±568	712±84	43722±2150	<7	41.5±11	<3
S311	26593±2040	5919±522	1846±137	28726±1420	<7	854.2±48	<3
S312	78914±4290	8118±610	1064±986	35858±1770	<7	88.2±13	<3
S313	20262±1530	5772±456	781±77	39056±1920	<7	98.6±12	45.1
S314	14663±1380	6678±504	902±81	37991±1860	69.7±11	<8	<3
S315	17062±1490	5799±478	858±87	42123±2070	<7	101.5±13	<3
S316	31859±2100	6159±489	594±73	30992±1525	<7	36.8±10	<3
S317	11297±1145	6518±476	838±81	56385±2760	<7	<8	<3

**Table 5.10: Metal pollution indexes for soil samples in Ndulukuni Hills**

Sample Code	Copper		Zinc		Lead	
	Conc. ( $\mu\text{g/g}$ )	Pollution index	Conc. ( $\mu\text{g/g}$ )	Pollution index	Conc. ( $\mu\text{g/g}$ )	pollution Index
S301	<7	-	<8	-	<3	-
S302	<7	-	<8	-	<3	-
S303	<7	-	75.2 $\pm$ 12	0.38	<3	-
S304	<7	-	124.0 $\pm$ 14	0.62	<3	-
S305	<7	-	174.2 $\pm$ 17	0.87	<3	-
S306	<7	-	82.8 $\pm$ 12	0.42	<3	-
S307	<7	-	95.5 $\pm$ 11	0.48	<3	-
S308	<7	-	143.4 $\pm$ 15	0.72	<3	-
S309	<7	-	164.9 $\pm$ 24	0.82	<3	-
S310	<7	-	41.5 $\pm$ 11	0.21	<3	-
S311	<7	-	854.2 $\pm$ 48	4.26	<3	-
S312	<7	-	88.2 $\pm$ 13	0.44	<3	-
S313	<7	-	98.6 $\pm$ 12	0.99	45.1 $\pm$ 9	0.45
S314	69.7 $\pm$ 11	0.93	<8	-	<3	-
S315	<7	-	101.5 $\pm$ 13	0.51	<3	-
S316	<7	-	36.8 $\pm$ 10	0.19	<3	-
S317	<7	-	<8	-	<3	-

## **Limestone**

Copper and zinc were below the detection limits of the in all the limestone samples analyzed. Lead was detected in 4 samples only with concentrations ranging from  $28.9 \mu\text{g/g} \pm 6$  to  $47.7 \mu\text{g/g} \pm 8$  and a mean value of  $34.4 \mu\text{g/g} \pm 9$ . The pollution indexes ranged from 0.29-0.45 with a mean value of 0.34.

Generally, the results indicated that soils in the region were not contaminated with heavy toxic metals. The mean calcium content of the limestone samples was found to be high approximately 32% of the ore by mass. It can therefore be concluded that the limestone rocks are not rich in heavy toxic elements; Cu, Zn and Pb similar to observations made in England (Kabata-Pendias and Pendias, 1984). The soil heavy metal content could thus be as a result of the bands of marble and granulites underlying the limestone outcrops (Xiangdong and Thorton 1993; Saggerson, 1957).

**Table 5.11: Average metal concentration for limestone samples from Ndulukuni Hill**

SAMPLE CODE	Ca	Ti	Mn	Fe	Cu	Zn	Pb
L301	198000±9450	<500	<100	420±49	<7	<8	<3
L302	223500±11000	<500	<100	468±61	<7	<8	28.9±6
L303	306750±16500	<500	<100	539±79	<7	<8	<3
L304	300000±13900	<500	<100	2145±133	<7	<8	<3
L305	327000±15200	<500	<100	599±69	<7	<8	<3
L306	273000±15500	<500	<100	596±82	<7	<8	47.7±8
L307	415500±20700	<500	<100	4485±249	<7	<8	<3
L308	339000±15600	<500	<100	2250±139	<7	<8	<3
L309	357000±18500	<500	<100	1186±109	<7	<8	<3
L310	246000±12900	<500	<100	4275±229	<7	<8	31.4±7
L311	342000±15400	<500	653±93	2115±131	<7	<8	<3
L312	280500±16400	<500	<100	915±90	<7	<8	<3
L313	319500±14600	<500	<100	1500±109	<7	<8	<3
L314	370500±17000	<500	<100	1085±99	<7	<8	<3
L315	421500±21300	<500	<100	579±95.8	<7	<8	<3
L316	343500±15600	<500	<100	<61.5	<7	<8	<3
L317	447000±21800	<500	<100	916±94.7	<7	<8	<3
L318	208500±9890	<500	240±59.6	453±53.4	<7	<8	<3
L319	384000±20500	<500	<100	590±89.8	<7	<8	<3
L320	472500±23000	<500	<100	1014±118	<7	<8	<3

**Table 5.12: Metal pollution indexes for limestone samples in Ndulukuni Hills**

Sample Code	Copper		Zinc		Lead	
	Conc. ( $\mu\text{g/g}$ )	Pollution index	Conc. ( $\mu\text{g/g}$ )	Pollution index	Conc. ( $\mu\text{g/g}$ )	pollution Index
L301	<7	-	<8	-	<3	-
L302	<7	-	<8	-	28.9 $\pm$ 6	0.29
L303	<7	-	<8	-	<3	-
L304	<7	-	<8	-	<3	-
L305	<7	-	<8	-	<3	-
L306	<7	-	<8	-	47.7 $\pm$ 8	0.48
L307	<7	-	<8	-	<3	-
L308	<7	-	<8	-	<3	-
L309	<7	-	<8	-	<3	-
L310	<7	-	<8	-	31.4 $\pm$ 7	0.31
L311	<7	-	<8	-	<3	-
L312	<7	-	<8	-	<3	-
L313	<7	-	<8	-	<3	-
L314	<7	-	<8	-	<3	-
L315	<7	-	<8	-	<3	-
L316	<7	-	<8	-	<3	-
L317	<7	-	<8	-	<3	-

## 5.2 Absorbed Dose Rates and Annual Effective Dose Rates.

The effective dose rates were measured using a survey meter and the annual effective dose rates and absorbed dose rates calculated from the results using conversion factors provided by UNSCEAR, 2000 as in equation 5.1

$$AED (mSvy^{-1}) = (ED (\mu Svy^{-1}) \times 24hrs /day \times 365days /yr \times K)/1000.....5.1$$

In which K is the outdoor occupancy factor and is equal to 4 and ED is the effective dose rate. The absorbed dose rates were calculated from the effective dose rate measurements at 1m above the ground level using a survey meter using conversion factor 0.7Sv/Gy as in equation 5.2;

$$AD(nGyh^{-1}) = ED(\mu Svh^{-1}) \times 10^3/0.7SvGy^{-1}.....5.2$$

Where AD is the absorbed dose and Ed effective dose

The calculated AEDs and absorbed dose rates were calculated from the activity concentrations of <sup>40</sup>K, <sup>232</sup>Th and <sup>238</sup>U per unit activity concentration for geological samples using the equation;

$$AD(nGyh^{-1}) = 0.621C_{Th} + 0.462C_U + 0.0417C_K.....5.3$$

### 5.2.1 Region 1(Kituvwi-Utekilawa Hills)

The average activity concentrations in Bq/Kg were;  $28.34 \pm 23$  with arrange of 8.6 – 105.9 for  $^{238}\text{U}$  and  $95.58 \pm 73$  with a range of 49.4 – 356.0 for  $^{40}\text{K}$  while  $^{232}\text{Th}$  was below detection limits.(Table ) The measured Annual Effective Dose rates (AEDs) were found to range from 0.598 to 0.947 mSv/h with a mean value of  $0.768 \text{ mSv/h} \pm 0.087$  which was below the maximum recommended dose limits for the general public of 1mSv/y. The absorbed doses were found to be ranging from 97.4 to 154.4 nGy/h with a mean value of  $125.3 \text{ nGy/h} \pm 14$ . This value is about two times the world's average absorbed dose of 60nGy/h implying that this region can be classified as High Level Natural Radiation Area (HLNRA).

The absorbed dose rates and the AEDs calculated from the activity concentrations showed a range of 6.3 nGy/h to 53.0 nGy/h with a mean of  $19.0 \text{ nGy/h} \pm 11$  and 0.015 to 0.13 mSv/y with an average of  $0.047 \text{ mSv/y} \pm 0.03$  respectively (Figures 5.1 and 5.2)

**Table 5.13: Activity concentrations for Limestone Samples from Kamaluu-Mwanyani Hills**

SAMPLE CODE	ACTIVITY CONCENTRATION (Bq/kg)	
	Uranium series ( $^{226}\text{Ra}$ )	Potassium ( $^{40}\text{K}$ )
L101	16.6	81.3
L102	19.8	65.6
L103	25.9	77.8
L104	19.7	53.3
L105	48.7	80.0
L106	9.1	56.9
L107	45.1	104.6
L108	25.0	74.1
L109	24.2	67.1
L110	8.6	60.4
L111	12.0	84.2
L112	22.1	94.5
L113	36.5	177.8
L114	30.8	61.0
L115	7.3	356
L116	24.5	80.8
L117	105.9	49.4
Mean	28.4 ± 23	95.6 ± 73
Range	8.6 – 105.9	49.4 – 356.0



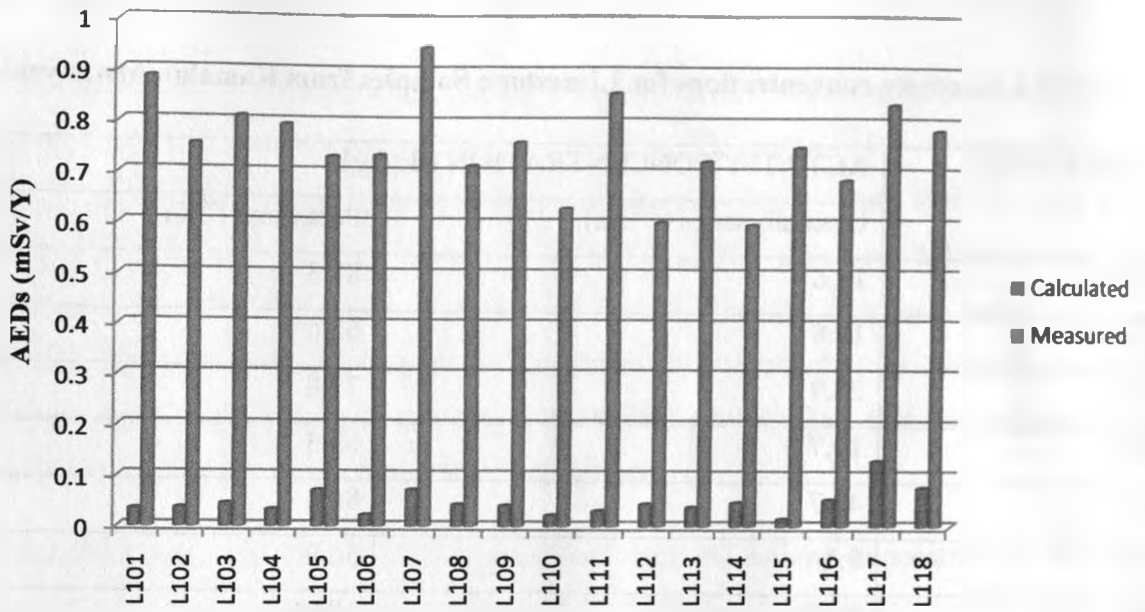


**Figure 5.1: Annual Effective Dose rates for Utekilawa-Kituvwi**

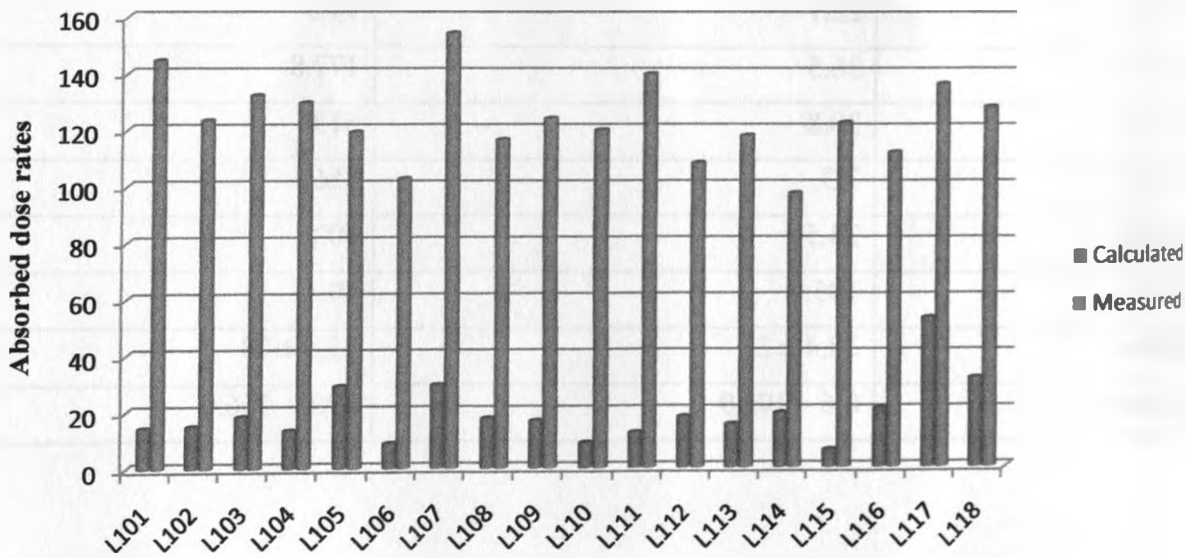


**Figure 5.2: Absorbed dose rates for Utekilawa-Kituvwi**

### 5.2.2 Region 2 (Kamaluu-Mwanyani Hills)

The activity concentrations in Bq/Kg of the limestone were found to have a range of 6.44 – 103.55 and an average of  $47.40 \pm 35$  for  $^{238}\text{U}$ , 38.79 – 481.37 and an average of  $142.63 \pm 127$  for  $^{40}\text{K}$  while  $^{232}\text{Th}$  was below detection limits. (Table 5.14). The measured AEDs were found to range from 0.666 to 1.262 mSv/y with a mean value of  $0.907 \pm 0.16$  which was below the maximum recommended dose limits for the general public of 1mSv/y. However, this value was very close to the maximum recommended dose thus little enrichment of the primordial radionuclides due to mining activities could cause exposure risks. The absorbed doses were found to range from 108.54 to 205.84 nGy/h with a mean value of  $147.82 \text{ nGy/h} \pm 25$ . This value is about 2.5 times the world's average absorbed dose of 60nGy/h thus the region can be classified as High Background Radiation Area (HBRA).

The absorbed doses calculated from the activity concentrations ranged from 8.34 to 67.72 nGy/h with a mean value of  $36.06 \text{ nGy/h} \pm 19$ . The AEDs calculated from the limestone activity concentrations ranged from 0.02 to 0.166 mSv/y with an average of  $0.088 \text{ mSv/y} \pm 0.05$  respectively which was found to be about 10% of the background AEDs. This could be attributed to the fact that measured values included cosmic radiations as well as secondary radiations from solar and other galactic events. The results are presented in figures 5.3 and 5.4

**Table 5.14 Activity Concentrations of Limestone Samples from Kamaluu-Mwanyani Hills**

SAMPLE CODE	ACTIVITY CONCENTRATION (Bq/kg)	
	<sup>238</sup> U Series ( <sup>226</sup> Ra)	Potassium ( <sup>40</sup> K)
L201	19.33	53.33
L202	99.41	55.31
L203	9.11	49.78
L204	50.63	71.11
L205	6.44	244.90
L206	78.24	379.25
L207	15.06	148.68
L208	13.56	38.79
L209	86.56	86.91
L210	88.87	142.22
L211	44.73	18.44
L212	103.55	156.44
L213	64.20	106.66
L214	13.11	154.07
L215	54.31	94.81
L216	11.31	481.36
Range	6.44 – 103.55	38.79 – 481.37
Mean	47.40 ± 35	142.63 ± 127

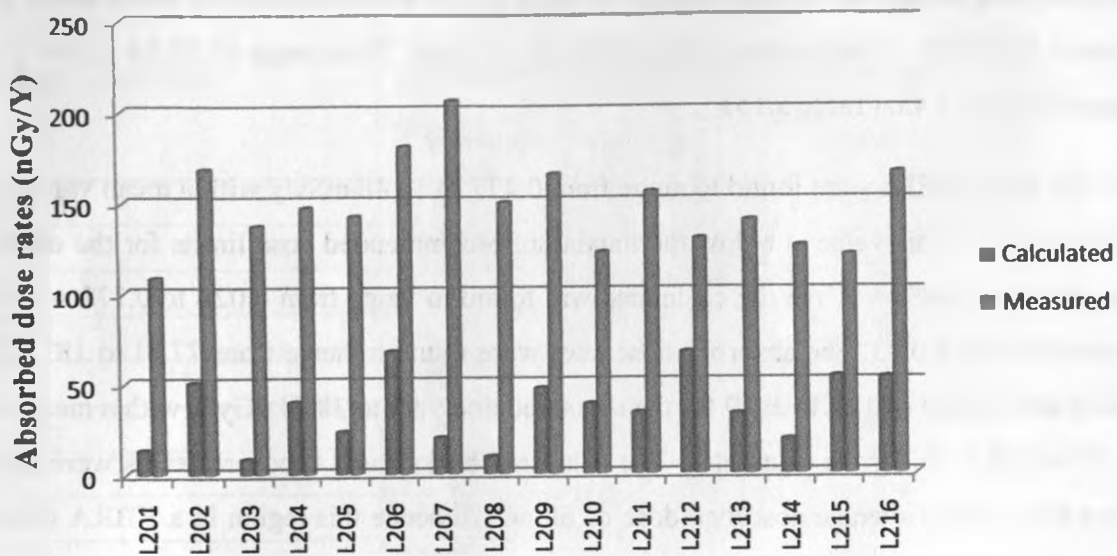


**Figure 5.3: Absorbed dose rates for Kamaluu-Mwanyani Hills**

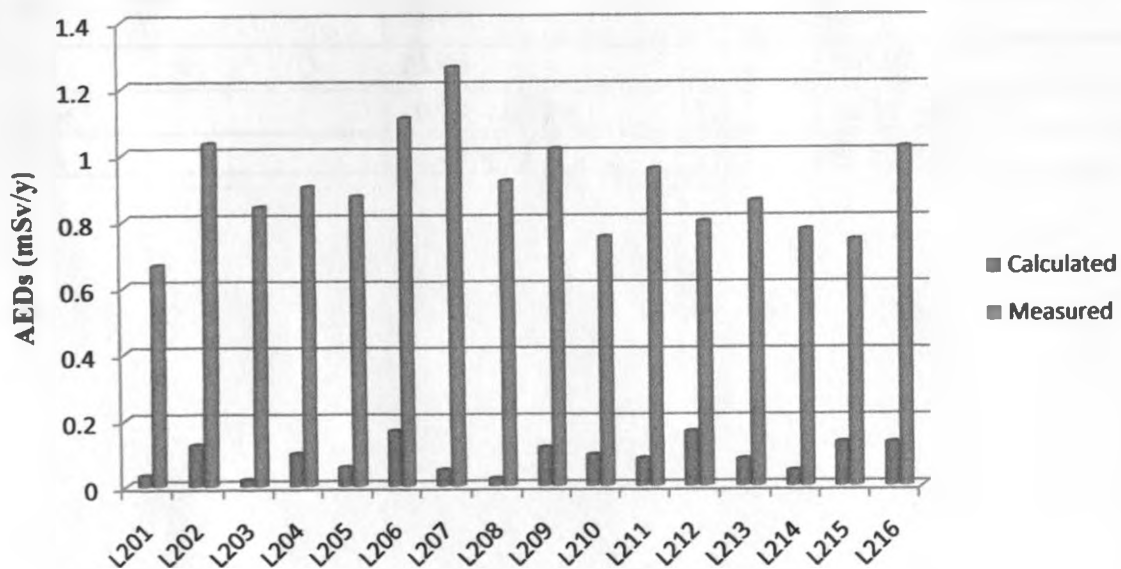


**Figure 5.4: Annual Effective Dose rates for Kamaluu-Mwanyani**

### 5.2.3 Region 3 (Ndulukuni Hills)

The samples had activity concentrations (Bq/Kg) of  $^{232}\text{Th}$  below detection limits while  $^{238}\text{U}$  had a range of 10.99 – 67.89 and a mean of  $32.24 \pm 17$  and  $^{40}\text{K}$  a range of 56.14 – 664.72 with a mean of  $87.35 \pm 43$ . (Table 5.15)

The measured AEDs were found to range from 0.477 to 1.148 mSv/y with a mean value of  $0.743 \text{ mSv/y} \pm 0.18$ . This value is below the maximum recommended dose limits for the members of the public of 1 mSv/y while the calculated were found to range from 0.024 to 0.178 with a mean value of  $0.064 \pm 0.03$ . The absorbed dose rates were found to range from 77.81 to 187.22 nGy/h giving an average of  $121.15 \pm 29$  for the measured and 9.90 to 38.74 nGy/h with a mean value of  $26.20 \text{ nGy/h} \pm 15$  for the calculated. The measured background exposure levels were about two times the world's average absorbed dose of 60 nGy/h hence this region is a HBRA (Figure 5.5 and 5.6)

**Table 5.15: Activity Concentrations of Limestone Samples from Ndulukuni Hills**

SAMPLE CODE	ACTIVITY CONCENTRATION (Bq/Kg)	
	<sup>238</sup> U Series ( <sup>226</sup> Ra)	Potassium ( <sup>40</sup> K)
L301	43.6	84.21
L302	43.08	56.89
L303	16	72.73
L304	10.99	58.05
L305	27.61	67.72
L306	67.89	88.89
L307	53.85	88.89
L308	12.35	56.14
L309	37.82	66.42
L310	19.39	60.52
L311	47.46	66.67
L312	15.06	64.04
L313	24.16	128.4
L314	17.49	205.43
L315	55.23	66.67
L316	23.93	165.92
Range	10.99 – 67.89	56.14 – 664.72
Mean	32.24 ± 17	87.35 ± 43

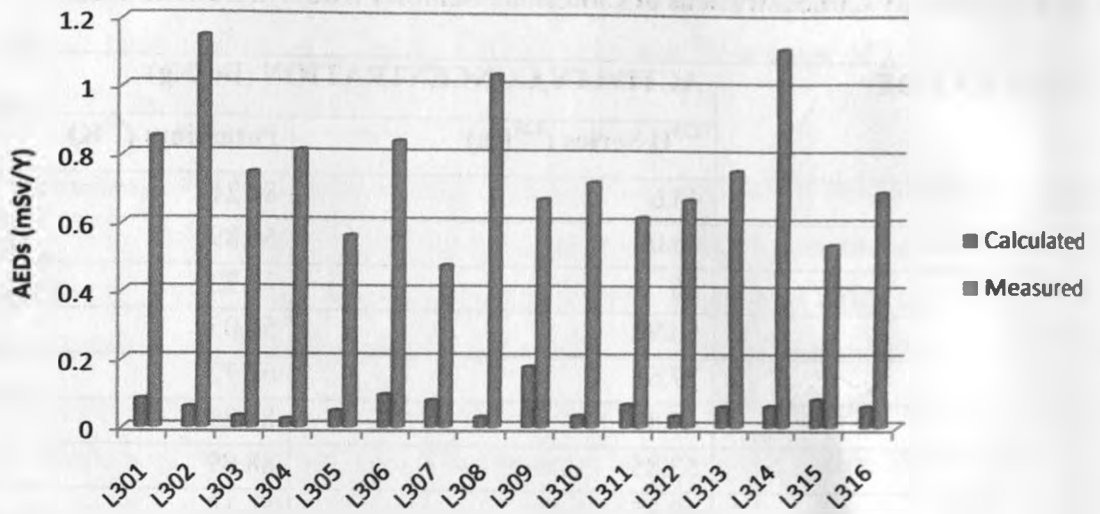


**Figure 5.5: Annual Effective dose rates for Ndulukuni Hills**

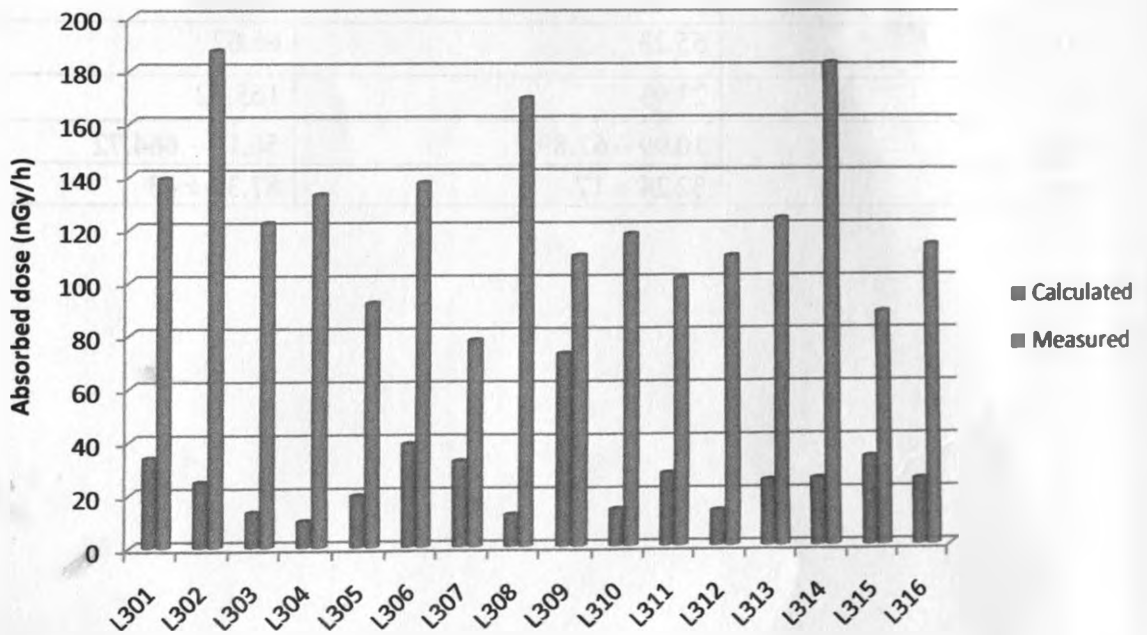


**Figure 5.6: Absorbed dose rates for Ndulukuni Hills**

A comparison of the measured and the calculated values in the three regions indicated a huge variation between the measured and the calculated values with the measured values being as high as 5 times the calculated values. This could be attributed to the fact that the measured values included cosmic radiations as well as secondary radiation from the solar and other galactic events. However, the contribution due to this is usually minimal since most cosmic rays are attenuated in the atmosphere (Rasolonjatovo et al 2002). This implies that the limestone samples could not be the sole source of the natural radioactivity in this region.

The high background radiation could therefore be attributed to the granulite rocks within the region as granites are associated with high concentration primordial radionuclides (UNSCEAR, 1993; Saggerson, 1957). Similar results were obtained in Uganda in the Kilembe copper-cobalt belt and Sukulu limestone deposits (Kisolo and Barifaijo, 2008).  $^{238}\text{U}$  was the major source of the background radiations with  $^{40}\text{K}$  contributing to a small percentage while  $^{232}\text{Th}$  was always below the detection limits of the equipment used. The results of this study concur with other studies in different parts of the world such as Canada and U. S. A, South Eastern Brazil and Nigeria (Carlos et al 2003; Wollenberg and Smith, 2008; Ademola, 2008).



## CHAPTER SIX

### 6.0 CONCLUSIONS AND RECOMENDATIONS

The concentrations of heavy metals Zn, Cu and Pb in both limestone and soil samples from the three regions making the limestone deposits of Kitui South have been determined using EDXRF technique. The concentrations of Zn, Cu and Pb in Utekilawa – Kituvwi hills were found to be below the U.S EPA soil metal pollution indexes of  $100\mu\text{g/g}$ ,  $75\mu\text{g/g}$  and  $200\mu\text{g/g}$  for Pb, Cu and Zn respectively. The mean values of the concentrations were  $49.60\mu\text{g/g} \pm 15$ ,  $79.80 \mu\text{g/g} \pm 27$  and  $31.7 \mu\text{g/g} \pm 10$  for Cu, Zn and Pb respectively. Limestone samples had metal concentrations below detection limits except for a few samples with mean values of  $187.50\mu\text{g/g} \pm 19$  for Cu. Zn was below detection limits for all the samples while Pb had a mean value of  $26.70 \mu\text{g/g} \pm 8$ . The soils and limestone in this region could be considered not to be contaminated with heavy metals Cu, Zn and Pb.

In Kamaluu-Mwanyani Hills, the metal concentrations were generally below the US. EPA soil metal limits with mean values being  $43.20 \mu\text{g/g} \pm 12$  for Cu,  $77.70 \mu\text{g/g} \pm 29$  for Zn and  $37.20 \mu\text{g/g} \pm 10$  for Pb in soil samples. Limestone samples in this region had Cu concentrations with an average of  $133.32 \mu\text{g/g} \pm 28$  which was above the soil Cu limits of  $75 \mu\text{g/g}$  thus contamination. The Zn concentrations had a mean value of  $92.61 \pm 32$  and the Pb average was  $32.39 \pm 9$ .

Soils from Ndulukuni Hills had an average concentration of  $99.32 \mu\text{g/g} \pm 42$  for Zn,  $69.70 \mu\text{g/g} \pm 11$  for Cu and  $45.00 \mu\text{g/g} \pm 9$  for Pb. Zn and Cu were below detection limits for all the limestone samples while Pb had an average concentration of  $34.40 \mu\text{g/g} \pm 9$ . Generally, soils and limestone from Kitui South were not contaminated with heavy metals Zn, Cu and Pb. However, precautions should be taken during the limestone mining and processing as the metal contents of soils seemed to originate from other rocks rather than limestone thus the tailings and water from mines may contain higher concentrations of these metals causing their enhancement.

The AEDs have also been measured and the absorbed dose rates calculated. The average AEDs were found to be  $0.768 \text{ mSv/yr} \pm 0.087$ ,  $0.907 \text{ mSv/yr} \pm 0.16$  and  $0.730 \text{ mSv/yr}$  for Utekilawa-Kituvwi Hills, Kamaluu-Mwanyani Hills and Ndulukuni Hills respectively. These values were

slightly below the maximum recommended dose limits for the public (1 mSv/yr). However, dumping of mine tailings and the mining processes may enhance the radionuclide concentrations causing increased exposure hence precautions must be taken during mining. The absorbed doses were found to be  $125.30 \text{ nGy/h} \pm 14$ ,  $147.82 \text{ nGy/h} \pm 25$  and  $121.15 \text{ nGy/y} \pm 29$  for Utekilawa-Kituvwi hills, Kamaluu-Mwanyani hills and Ndulukuni Hills respectively. All these values were about 2 times the global exposure rates thus this area can be classified as HBRA.

The activity concentrations of the radionuclides from limestone have also been determined using HPGe and the exposure and absorbed dose rates and AEDs calculated. The results indicated that the highest activity was mainly from  $^{238}\text{U}$  with some concentrations from  $^{40}\text{K}$  while  $^{232}\text{Th}$  was below detection limits. The average activity concentrations in Bq/Kg were;  $28.34 \pm 23$ ,  $47.40 \pm 36$  and  $32.24 \pm 18$  for  $^{238}\text{U}$  and  $95.58 \pm 73$ ,  $142.63 \pm 127$  and  $87.35 \pm 43$  for  $^{40}\text{K}$  for Utekilawa-Kituvwi Hills, Kamaluu-Mwanyani Hills and Ndulukuni Hills respectively. The AEDs and absorbed doses were  $0.047 \text{ mSv/y} \pm 0.03$ ,  $19.04 \text{ nGy/h} \pm 11$  for utekilawa-Kituvwi Hills,  $0.088 \text{ mSv/y} \pm 0.05$  and  $36.06 \text{ nGy/h} \pm 19$  for kamaluu-Mwanyani Hills and  $0.064 \text{ mSv/y} \pm 0.04$  and  $26.20 \text{ nGy/h} \pm 15$  for Ndulukuni Hills respectively. These values are far below the maximum recommended AED for the general public hence the limestone samples were found to pose no exposure risks when used for manufacture of building materials such as cement. The study did not include the determination of exposure due to radon and its progeny, level of natural radionuclides in water as well as the ambient air quality thus the need for further studies on these. Studies on background radiation exposure, radionuclide concentrations and heavy metal concentrations of the soils and the surroundings should also be done regularly during and after the mining and processing of limestone in the area in order to monitor its effects on the local environment.

## CHAPTER SIX

### 6.0 CONCLUSIONS AND RECOMENDATIONS

The concentrations of heavy metals Zn, Cu and Pb in both limestone and soil samples from the three regions making the limestone deposits of Kitui South have been determined using EDXRF technique. The concentrations of Zn, Cu and Pb in Utekilawa – Kituvwi hills were found to be below the U.S EPA soil metal pollution indexes of  $100\mu\text{g/g}$ ,  $75\mu\text{g/g}$  and  $200\mu\text{g/g}$  for Pb, Cu and Zn respectively. The mean values of the concentrations were  $49.60\mu\text{g/g} \pm 15$ ,  $79.80 \mu\text{g/g} \pm 27$  and  $31.7 \mu\text{g/g} \pm 10$  for Cu, Zn and Pb respectively. Limestone samples had metal concentrations below detection limits except for a few samples with mean values of  $187.50\mu\text{g/g} \pm 19$  for Cu. Zn was below detection limits for all the samples while Pb had a mean value of  $26.70 \mu\text{g/g} \pm 8$ . The soils and limestone in this region could be considered not to be contaminated with heavy metals Cu, Zn and Pb.

In Kamaluu-Mwanyani Hills, the metal concentrations were generally below the US. EPA soil metal limits with mean values being  $43.20 \mu\text{g/g} \pm 12$  for Cu,  $77.70 \mu\text{g/g} \pm 29$  for Zn and  $37.20 \mu\text{g/g} \pm 10$  for Pb in soil samples. Limestone samples in this region had Cu concentrations with an average of  $133.32 \mu\text{g/g} \pm 28$  which was above the soil Cu limits of  $75 \mu\text{g/g}$  thus contamination. The Zn concentrations had a mean value of  $92.61 \pm 32$  and the Pb average was  $32.39 \pm 9$ .

Soils from Ndulukuni Hills had an average concentration of  $99.32 \mu\text{g/g} \pm 42$  for Zn,  $69.70 \mu\text{g/g} \pm 11$  for Cu and  $45.00 \mu\text{g/g} \pm 9$  for Pb. Zn and Cu were below detection limits for all the limestone samples while Pb had an average concentration of  $34.40 \mu\text{g/g} \pm 9$ . Generally, soils and limestone from Kitui South were not contaminated with heavy metals Zn, Cu and Pb. However, precautions should be taken during the limestone mining and processing as the metal contents of soils seemed to originate from other rocks rather than limestone thus the tailings and water from mines may contain higher concentrations of these metals causing their enhancement.

The AEDs have also been measured and the absorbed dose rates calculated. The average AEDs were found to be  $0.768 \text{ mSv/yr} \pm 0.087$ ,  $0.907 \text{ mSv/yr} \pm 0.16$  and  $0.730 \text{ mSv/yr}$  for Utekilawa-Kituvwi Hills, Kamaluu-Mwanyani Hills and Ndulukuni Hills respectively. These values were

slightly below the maximum recommended dose limits for the public (1 mSv/yr). However, dumping of mine tailings and the mining processes may enhance the radionuclide concentrations causing increased exposure hence precautions must be taken during mining. The absorbed doses were found to be  $125.30 \text{ nGy/h} \pm 14$ ,  $147.82 \text{ nGy/h} \pm 25$  and  $121.15 \text{ nGy/h} \pm 29$  for Utekilawa-Kituvwi hills, Kamaluu-Mwanyani hills and Ndulukuni Hills respectively. All these values were about 2 times the global exposure rates thus this area can be classified as HBRA.

The activity concentrations of the radionuclides from limestone have also been determined using HPGe and the exposure and absorbed dose rates and AEDs calculated. The results indicated that the highest activity was mainly from  $^{238}\text{U}$  with some concentrations from  $^{40}\text{K}$  while  $^{232}\text{Th}$  was below detection limits. The average activity concentrations in Bq/Kg were;  $28.34 \pm 23$ ,  $47.40 \pm 36$  and  $32.24 \pm 18$  for  $^{238}\text{U}$  and  $95.58 \pm 73$ ,  $142.63 \pm 127$  and  $87.35 \pm 43$  for  $^{40}\text{K}$  for Utekilawa-Kituvwi Hills, Kamaluu-Mwanyani Hills and Ndulukuni Hills respectively. The AEDs and absorbed doses were  $0.047 \text{ mSv/y} \pm 0.03$ ,  $19.04 \text{ nGy/h} \pm 11$  for Utekilawa-Kituvwi Hills,  $0.088 \text{ mSv/y} \pm 0.05$  and  $36.06 \text{ nGy/h} \pm 19$  for Kamaluu-Mwanyani Hills and  $0.064 \text{ mSv/y} \pm 0.04$  and  $26.20 \text{ nGy/h} \pm 15$  for Ndulukuni Hills respectively. These values are far below the maximum recommended AED for the general public hence the limestone samples were found to pose no exposure risks when used for manufacture of building materials such as cement. The study did not include the determination of exposure due to radon and its progeny, level of natural radionuclides in water as well as the ambient air quality thus the need for further studies on these. Studies on background radiation exposure, radionuclide concentrations and heavy metal concentrations of the soils and the surroundings should also be done regularly during and after the mining and processing of limestone in the area in order to monitor its effects on the local environment.

## REFERENCES

- Achola, S. O (2009).** Radioactivity and elemental analysis of carbonite rocks from parts of Gwasi area, south western Kenya. *M.Sc. Thesis, University of Nairobi, Unpublished.*
- Aly Abdo, A.A., Hassan, M.H. and Huwait, M.R.A (1999).** Radioactivity assessment of fabricated phosphogypsum mixtures. *Fourth Radiation Physics Conference, 15–19 November 1999, Alexandria, Egypt: pp. 632–640.*
- Bigu, J., Mohamed, I. H. and Hussein, A. Z (2000).** Radiation measurements in Egyptian pyramids and tombs-occupational exposure of workers and the public. *Journal of Environmental Radioactivity 47: pp. 245-252.*
- Boularbah, A., Schwartz, C., Bitton, G. and Morel J. L (2006).** Heavy metal contamination from mining sites in South Morocco: Use of a biotest to assess metal toxicity of tailings and soil. *Chemosphere 63: pp. 802-810.*
- Conesa, H. M., Faz, A. and Raquel, A (2006).** Heavy metal accumulation and tolerance in plants from mine tailings of the semi arid Cartagena La- Union mining district (SE Spain). *Science of the total environment 366: pp. 1-11.*
- David, C. P. (2003).** Heavy metal concentration in growth bands of corals: a record of mining tailings input through time (Marinduque Island, Philippines). *Marine Pollution Bulletin 46: pp. 187-196.*
- Dodson, R. G (1953).** A geology of south east machakos area. *Geol. Surv. Kenya. Report No. 25: pp.3*
- Dudka, S. and Adriano, C. D (1997).** Environmental impacts of metal ore mining and processing. *J. Environ. Qual. 26: 590-602.*

**European Commission (EC), (2002).** Practical use of the concepts of clearance and exemption and exemption, Part II, application of the concepts of exemption and clearance of natural radiation sources. *Radiation Protection vol 122. Part II (Luxembourg: EC).*

**Funtua, I. I. and Elegba, S. B (2005).** Radiation exposure from high-level radiation area and related mining and processing activities of Jos Plateau, central Nigeria. *International Congress Series 1276: pp. 401– 402.*

**Gregory, R. L (1992).** Analytical electron microscopy of Columbite: A niobium-tantalum oxide mineral with zonal uranium distribution. *Journal of Nuclear Materials 190 North-Holland: pp. 302-311.*

**Karakelle, B., Ozturk, N., Kose, A., Varinlioglu, A., Erkol, A. Y and Yilmaz, F (2002).** Natural radioactivity in soil samples of kocaali basin, Turkey. *J. Radioanal. Nucl. Chem. 254: 649-651.*

**Khan, H. A., Qureshi, I. E. and Tufail, M (1993).** Passive dosimetry of Radon and its daughters using solid state nuclear track detectors (SSNTDs). *Radiation protection dosimetry, 46: 149-170.*

**Gupta, C. K. and Suri A. K (1994).** Extractive Metallurgy of Niobium, *CRC Press, USA: pp. 21-121.*

**Habashi, F (1997).** Handbook of Extractive Metalurgy, *vol. 3, Wiley-VCH, Germany: pp. 1404-1421.*

**Henriques, F. S. and Fernandes, J. C (1991).** Metal uptake and distribution in rush (*Juncus Conglomeratus*) plants growing in pyrites mine tailings at Lousal, Portugal. *Sci. Total Environ. 102: 253-260.*

**International Atomic Energy Agency (IAEA), (2004).** Application of the Concepts of Exclusion, Exemption and Clearance. *Safety Series No. RS-G-1.7 (Vienna: IAEA).*

**Ibrahiem, N.M., Abdel-Ghani, A.H., Shawky, S.M., Ashraf, E.M. and Farouk, M.A (1993).** Measurement of radioactivity levels in soil in the Nile Delta and Middle Egypt. *Health Phys. 64: pp. 620–627.*

**International Commission on Radiation Protection (ICRP), (1991).** Recommendations of the International Commission on Radiological Protection *ICRP Publication 60; Ann. ICRP 21 (1–3), Pergamon Press, Oxford.*

**International Commission on Radiation Protection (ICRP), (2000).** Protection of the public in situations of prolonged radiation exposure *ICRP Publication 82; Ann. ICRP 29 (1–2), Pergamon Press, Oxford.*

**Juhász, L., Serbin, P. and Czoch, I (2005).** Evaluation of technologically enhanced naturally occurring radioactive materials in Hungary. *International congress series. 1276: 367-368.*

**Ludewig, P. and Lorensen, E (1924).** Investigation of air in Schneeberg-Obserchlema Boring for rado emanation content. *Phyikalle Zeltscher, 22: 178-185.*

**Malance, A., Gaidolfi, L., Pessina, V. and Dallara, G (1996).** Distribution of  $^{226}\text{Ra}$ ,  $^{232}\text{Th}$  and  $^{40}\text{K}$  in soils of Rio Grande do Norte, Brazil. *J. Environ. Radioactiv. 30: pp. 55–67.*

**Mangala, J. M (1987).** A multi-channel X-ray fluorescence analysis of flourspar ore and rock from Mrima hill, Kenya, *MSc Thesis, University of Nairobi.*

**Mbuzukongira, P (2006).** Assessment of occupational radiation exposures of artisan miners of Columbite-tantalite (Coltan) in the Eastern Democratic Republic of Congo. *MSc Thesis, University of Nairobi, Unpublished.*

**McCall, G. J. H (1958).** Geology of Gwasi area, Ministry of Commerce and Industry. *Geology Survey of Kenya Dept. No.45.*

**Mustapha, A. O (1999).** Assessment of human exposures to natural sources of radiation in Kenya. *Ph.D Thesis, University of Nairobi, Unpublished.*

**Mbuzukongira, P., Mustapha, A.O. and Mangala, M. J (2007).** Occupational radiation exposures of artisans mining Columbite-tantalite in the eastern Democratic Republic of Congo, *J. Radiol. Prot. 27: pp. 187-195.*

**Mustapha, A.O., Patel, J.P. and Rathore, I.V.S (2002).** Preliminary report on radon concentration in drinking water and indoor air in Kenya. *Environmental Geochemistry and health 24(4): pp. 387-396.*

**National Council on Radiation Protection (NCRP) (1993).** Limitation of exposure to ionizing radiation, *NCRP Report No.116, Bethesda, MD.*

**Nazaroff, W. W. and Nero jr, A. V (1988).** Radon and its decay products in air. *New York. Wiley.*

**Odumo, B. O (2009).** Radiological survey and elemental analysis in the gold mining belt, southern Nyanza, Kenya, *M.Sc Thesis, University of Nairobi, Unpublished.*

**Patel, J. P (1991).** Environmental radiation survey of the area of high natural radioactivity of Mrima hill of Kenya. *Discovery and innovation 3(3): pp. 31-36.*

**Qureshi, A. A., Kakar, D. M., Akran, M., Khattak, M. T., Mehmood, K. and Khan, H. A (2000).** Radon concentrations in coal mines of Baluchistan, Pakistan. *Journal of Environmental Radioactivity 48: 203-209.*



**Rodriguez, L., Ruiz, E., Alonso, A. J. and Rincon, J (2009).** Heavy metal distribution and chemical speciation in tailings and soils around a Pb-Zn mine in Spain. *Journal of environmental management* 90: pp. 1106-1116.

**Saggerson, E. P (1957).** Geology of the Kitui south area. *Geol. Surv. Kenya. Degree sheet No. 53; south west quarter.*

**Sanders, L. D (1954).** Geology of the Kitui area. *Geol. Surv. Kenya. Report No. 30.*

**Sherman, J.,(1955).** *Spectrochim. Acta.* 7, 283.

**Stewart, C. G. and Simpson, S. D (1964).** Radiological health and safety in mining and milling of nuclear materials. *ATI/PUB/78, Viena, 1: 333.*

**Tsai, T. L., Lin, C. C., Wang, T. W and Chu, T. C (2008).** Radioactivity concentrations and dose assessment for soil samples around a nuclear power plant IV in Taiwan. *J. Radiol. Prot.* 28: 347-360.

**Tzortzis, M., Svoukis, E. and Tsertos, H (2004).** A comprehensive study of natural gamma radioactivity levels and associated dose rates from surface soils in Cyprus. *Radiat. Prot. Dosim.* 109: 217-224.

**United Nations Scientific Committee on the Effects of Atomic Radiation (UNSCEAR) (1998).** Sources and effects of ionization radiation Report to the General Assembly, with Scientific Annexes B: Exposures from Natural Radiation Sources (New York: UNSCEAR).

**United Nations Scientific Committee on the Effects of Atomic Radiation (UNSCEAR) (2000).** Sources, effects and risks of ionization radiation, Report to The General Assembly, with Scientific Annexes B: Exposures from Natural Radiation Sources (New York: UNSCEAR).

**United Nations Scientific Committee on the Effects of Atomic Radiation (UNSCEAR), (2008).** Sources and Effects of Ionizing Radiation, Report of the United Nations Scientific Committee on the Effects of Atomic Radiation, Fifty-sixth session, New York, USA.

**Varley, N. R. and Flowers, A. G (1998).** Indoor radon prediction from soil gas measurements. *Health Physics.* 74: 714-718.

**Wong, M. H (2003).** Ecological restoration of mine degraded soils with emphasis on metal contaminated soils. *Chemosphere.* 50: 775-780.

**Wong, J. W. C., Ip, C. M. and Wong, M. H (1998).** Acid forming capacity of Pb-Zn mine tailings and its implications for mine rehabilitation. *Environ. Geochem. Health.* 20: 149-155.

## APPENDICES

**Appendix 1: Absorbed Dose (nGy/h) and Annual Effective Doses (AED) for Samples from Utekilawa-Kituvwi Hills**

Sample code	Absorbed Dose (nGy/h)		Annual Effective Dose (mSv/y)	
	Calculated	Measured	Calculated	Measured
L101	14.4	144.7	0.035	0.887
L102	15.0	123.4	0.037	0.756
L103	18.4	132.3	0.045	0.811
L104	13.5	129.6	0.033	0.795
L105	29.1	119.2	0.071	0.731
L106	8.9	102.7	0.022	0.735
L107	29.5	154.4	0.072	0.947
L108	17.7	116.5	0.043	0.714
L109	16.8	124.0	0.041	0.761
L110	9.0	119.9	0.022	0.630
L111	12.5	139.9	0.031	0.858
L112	18.1	108.2	0.044	0.603
L113	15.4	117.9	0.038	0.723
L114	19.3	97.4	0.047	0.598
L115	6.3	122.5	0.015	0.751
L116	21.0	111.9	0.053	0.686
L117	53	136.4	0.130	0.836
L118	31.6	128.1	0.077	0.785
Average	19.04 ± 11.3	125.3 ± 14.1	0.047 ± 0.03	0.768 ± 0.09

**Appendix 2: Absorbed Dose and AEDs for Limestone Samples from Kamaluu-Mwanyani Hills**

Sample code	Absorbed Dose (nGy/h)		Annual Effective Dose (mSv/y)	
	Calculated	Measured	Calculated	Measured
L201	13.36	108.54	0.033	0.666
L202	50.52	168.30	0.124	1.032
L203	8.34	137.14	0.02	0.841
L204	39.86	147.13	0.098	0.902
L205	23.31	142.31	0.057	0.873
L206	67.62	180.76	0.166	1.108
L207	19.94	205.84	0.049	1.262
L208	9.48	149.83	0.023	0.919
L209	47.19	165.51	0.116	1.015
L210	38.51	122.34	0.094	0.750
L211	33.65	155.77	0.083	0.955
L212	67.03	129.86	0.164	0.796
L213	32.96	139.89	0.081	0.858
L214	18.85	125.81	0.046	0.771
L215	53.43	120.60	0.131	0.740
L216	52.86	166.09	0.13	1.018
Range	8.34 – 67.72	108.54 – 205.84	0.020 - 0.166	0.666 – 1.262
Mean	36.06 ± 19	147.82 ± 25	0.088 ± 0.05	0.907 ± 0.16

### Appendix 3: Absorbed Dose and AEDs for Limestone Samples from Ndulukuni Hills

Sample code	Absorbed Dose (nGy/h)		Annual Effective Dose (mSv/y)	
	Calculated	Measured	Calculated	Measured
L301	33.66	138.93	0.083	0.852
L302	24.62	187.22	0.06	1.148
L303	13.25	122.19	0.033	0.749
L304	9.9	132.90	0.024	0.815
L305	19.43	91.95	0.048	0.564
L306	38.74	137.29	0.095	0.842
L307	32.25	77.81	0.079	0.477
L308	12.08	169.23	0.03	1.038
L309	72.64	109.65	0.178	0.672
L310	13.98	117.71	0.034	0.722
L311	27.46	100.97	0.067	0.619
L312	13.33	109.36	0.033	0.671
L313	24.62	123.49	0.06	0.757
L314	25.13	182.35	0.062	1.118
L315	33.26	88.04	0.082	0.540
L316	24.83	113.36	0.061	0.695
Range	9.90 – 38.74	77.81 – 187.22	0.024 – 0.178	0.477 – 1.148
Mean	26.20 ± 15	121.15 ± 29	0.064 ± 0.03	0.743 ± 0.18